DIRECT DETECTION OF DIGITAL OPTICAL COMMUNICATION THROUGH THE ATMOSPHERE

by

David F. Chang

Submitted to the Faculty of the Oregon Graduate Center in partial fulfillment of the requirements for the degree of Master of Science.

Oregon Graduate Center

1974

This Master's Thesis has been examined by a committee of the Oregon Graduate Center as follows:

Charles M. McIntyre
Assistant Professor
Thesis Advisor

Douglas F. Barofsky
Associate Professor

Richard A. Elliott
Assistant Professor

Thomas M. Loehr
Associate Professor

ACKNOWLEDGMENTS

I would like to express my deep appreciation to Dr. Charles McIntyre for his help, guidance and patience throughout the duration of this research. Thanks also to Dr. Douglas Barofsky, Dr. Richard Elliott, and Dr. Thomas Loehr for their repeated reviewing of this thesis. Also my sincere thanks to my wife Paulina who not only typed and retyped many drafts of this thesis but also brought a baby to the family.

TABLE OF CONTENTS

I. INTRODUCTION

Coherent optical communication systems are fundamentally of interest because of the high achievable antenna gains, enormous potential information rates, privacy and security of the link, and other advantages relating to particular-link geometries. The antenna-gain advantage, which is proportional to λ^{-2} is especially important in long-range situations or where compact equipment is required.[1]

Because there are windows in the atmosphere in the visible wavelength range and in the near infrared around 2μm, 3.5μm, and between 8μm and 12μm[2], the atmosphere is also an important channel for coherent optical communication systems. But the atmosphere can severely degrade performance through the effect of turbulence.

The effect of the atmosphere on laser radiation includes scattering due to fog and rain, beam wander and spread, amplitude scintillation and wave front distortion. The effect of scattering can be partially overcome through the use of longer wavelengths, higher power and wide-field-of-view receivers[3]. Beam wander and (instantaneous) spread as a function of optical and turbulence parameters may be cancelled by using larger beam sizes at the receiver. There remains the effects of clear air turbulence: amplitude scintillation and wave front distortion.

There are two basic types of receivers in optical systems for communication through the atmosphere. Direct detection receivers[4] are favored at visible or near infrared wavelengths, and they have the advantage of the availability of sensitive, room-temperature detectors. Optical heterodyne receivers[4] are favored at middle-infrared wavelengths.

Direct detection receivers are affected by beam wander and scintillation. Beam wander can be largely cancelled as mentioned before.

Scintillation remains as the primary effect that degrades the performance of a direct detection optical communication link in the atmosphere. At a point in the receiver plane, the received field amplitude can be modeled as a log normal random variable. If a "point" detector (small with respect to the characteristic size of the scintillating amplitude patches) is placed in the received field, the photocurrent is observed to vary in time with a dynamic range that can approach 80 db. Typically, this large variation in the photocurrent may be reduced by using a large aperture receiver (large compared with the scintillating amplitude patches) so that, in effect, a spatial average over many independent patches is performed (e.g. if the aperture is as large as the beam, then from energy considerations, it is clear that the total fading is small). In particular, the variance in the photocurrent can be reduced by adding together N independent signals. If σ^2 represents the variance

for a single signal, then the total variance in a simple additive processor will be σ^2/N.

For a log normal process the dynamic range of fading is approximately

$$\text{db (fading)} \approx 100 \times \text{(variance)}$$

so that the fading can be reduced dramatically by averaging over a few independent signals. Conditions, such as strong turbulence and a large beam in the receiver plane, reduce the effectiveness of "aperture averaging". The reason is that the amplitude patches are not truly independent in such a case. Residual correlations extending over tens of centimeters have been measured (see Sec. II). Under these conditions, the optimum receiver consists of an array of collectors separated by distances large enough to ensure independence.

In this work direct detection at a visible wavelength (4880Å) is being investigated with three kinds of receivers: (1) a photon bucket (large aperture receiver), (2) a four element array with electronic processing (linear addition and nonlinearly weighted addition), and (3) a four element array with optical processing (linear addition).

During the preliminary experimental work, it was discovered that the results from the optical processing and the linear electronic processing were very similar. However, the signal-to-noise ratio was better using the electronic processing (due to the attenuation of the

signals in the optical fibers in the optical processing) and, consequently, the primary effort in this work is devoted to a comparison of the four element array with electronic processing and the photon bucket.

In Section II, the theoretical predictions of the variance for linear addition and weighted addition of signals are described in detail. The relation between bit-error-rate and signal to noise ratio is described analytically. In Section III, the experimental work is described. A discussion of the results and conclusions of this thesis will be stated in Sections IV and V.

II. THEORY

The effects of the atmosphere on an optical beam have been treated in some detail[5,6,7], and experimental evidence verifying these theories and establishing the region of their validity has been developed.[8] As a result, in clear air turbulence, the random distribution of beam amplitude can be approximated by a log normal probability density function. A characteristic of the log normal distribution is that there is a relatively high probability that the random variable will take on values that are far removed from the mean. It is this characteristic that accounts for the deep fades[5] that may contribute to the poor performance of optical links in the atmosphere

It is known that under some conditions, the technique of using a receiver that is large compared to the size of the scintillating amplitude patches works poorly.[8,9] A suitably spaced array works better provided that the receiving aperture receives a number N of statistically independent portions of the pattern corresponding to the predominant scale size. Then the log-intensity variance of the received signal will be reduced by a factor N.[5,10,11,12] This can improve the performance of an optical communications link over that which can be expected from a simple receiver.

In addition to the physical configuration of the receiver, there arises the question of how to process the resulting signals. In particular, how should the individual signals from the array elements be combined to optimize the performance of the link? A straight forward analysis given in Appendix II indicates that under certain conditions the optimum processing is to square the individual signals and then add them. In a comparison of the following three receivers

1. Photon bucket
2. 4 element array with electronic processing
3. 4 element array with optical processing (the four received signals are optically added by using fiber optics to superimpose the signals on a single detector)

it is both interesting and useful to note that in each case, the resulting signals are log normal, with means and variances that may be computed as shown below.

Consider the optical irradiance from a single element to be described by

$$I(x_i) = I_o e^{2\ell(x_i)}$$

where $\ell(x_i)$ is a normally distributed random variable with mean η_ℓ and variance σ_ℓ^2 ; and x_i is the position of the ith detector. Note that

$$\langle I(x_i) \rangle = I_o$$

where I_o is the irradiance that would be observed in the absence of scintillation. This requires that

$$\langle e^{2\ell(x_i)} \rangle = 1$$

and consequently that

$$\eta_\ell = -\sigma_\ell^2 \,*$$

In the discussion that follows, subscripts will be used to denote which random variable the statistical averages are applied to, e.g.,

$$\eta_{I_i} = \langle I(x_i) \rangle$$

$$\sigma_{I_i}^2 = \langle [I(x_i) - \langle I(x_i) \rangle]^2 \rangle$$

*This is in essence a conservation of energy requirement and is discussed in Ref. 6, 11.

and

$$\eta_{\ln I_i} = \langle \ln I(x_i) \rangle$$

Now define the random variable

$$I_1(x) = \frac{1}{N} \sum_{i=1}^{N} I(x_i)$$

corresponding to the irradiance that would be observed from an equivalent detector after simply summing the signals. Then

$$\begin{aligned} \eta_{I_1} &= \left\langle \frac{1}{N} \sum_{i=1}^{N} I(x_i) \right\rangle \\ &= \frac{1}{N} \left\langle \sum_{i=1}^{N} I_0 e^{2\ell(x_i)} \right\rangle \\ &= \frac{I_0}{N} \sum_{i=1}^{N} \left\langle e^{2\ell(x_i)} \right\rangle \\ &= I_0 \end{aligned}$$

Similarly,

$$\begin{aligned} \sigma_{I_1}^2 &= \left\langle \left[\frac{1}{N} \sum_{i=1}^{N} I(x_i) - \left\langle \frac{1}{N} \sum_{i=1}^{N} I(x_i) \right\rangle \right]^2 \right\rangle \\ &= \frac{I_0^2}{N^2} \left\langle \left[\sum_{i=1}^{N} \sum_{j=1}^{N} e^{2\ell(x_i)} e^{2\ell(x_j)} - 2 \sum_{i=1}^{N} e^{2\ell(x_i)} \left\langle \sum_{i=1}^{N} e^{2\ell(x_i)} \right\rangle \right.\right. \\ &\qquad \left.\left. + \left\langle \sum_{i=1}^{N} e^{2\ell(x_i)} \right\rangle^2 \right] \right\rangle \\ &= \left(\frac{I_0}{N}\right)^2 \left\langle \sum_{i=1}^{N} e^{4\ell(x_i)} + 2 \sum_{i \neq j}^{N} \sum_{j=1}^{N} e^{2[\ell(x_i) + \ell(x_j)} - N^2 \right\rangle \\ &= \left(\frac{I_0}{N}\right)^2 \left\{ N e^{4\sigma_\ell^2} - N^2 + 2 \sum_{i \neq j}^{N} \sum_{j=1}^{N} e^{4 C_\ell(\rho_{ij})} \right\} \end{aligned}$$

where

$$C_\ell(\rho_{ij}) = \langle [\ell(x_i) - \langle \ell(x_i) \rangle][\ell(x_j) - \langle \ell(x_j) \rangle] \rangle$$

$$\rho_{ij} = |x_i - x_j|$$

$$C_\ell(0) = \sigma_\ell^2$$

Note that for N = 1, a single detector,

$$\eta_{I_i} = I_0$$

$$\sigma_{I_i}^2 = I_0^2 (e^{4\sigma_\ell^2} - 1)$$

Also note that for the uncorrelated case, i.e., $C_\ell(\rho_{ij}) = 0$ when $i \neq j$, that

$$\sigma_{I_1}^2 = \frac{I_0^2}{N} (e^{4\sigma_\ell^2} - 1)$$

In a similar manner (See Appendix I), it can be shown that for a random variable defined by

$$I^2(x) = \frac{1}{N} \sum_{i=1}^{N} I^2(x_i)$$

corresponding to squaring before adding;

$$\eta_{I^2} = I_0^2 \, e^{4\sigma_\ell^2}$$

and

$$\sigma_{I^2}^2 = \frac{I_0^4}{N^2} \left\{ N e^{24\sigma_\ell^2} - N^2 e^{8\sigma_\ell^2} + 2 \sum_{i \neq j}^{N} \sum_{j=1}^{N} e^{8[\sigma_\ell^2 + 2C_\ell(\rho_{ij})]} \right\}$$

and 2, respectively, as a function of N, with $\sigma_\ell 2$ as a parameter. The reduction in the variance of the log irradiance as the number of elements is increased is clearly illustrated. Note, in particular, that in all cases $\sigma^2_{\ln I^2}$ is greater than $\sigma^2_{\ln I_1}$, although under certain conditions (as described in Appendix II) the performance of the communication

TABLE I

	η (MEAN)		σ^2 (VARIANCE)	
	CORRELATED CASE	INDEPENDENT CASE	CORRELATED CASE	INDEPENDENT CASE
$I(x_i)$	I_0	I_0	$I_0^2 (e^{4\sigma_\ell^2} - 1)$	$I_0^2 (e^{4\sigma_\ell^2} - 1)$
$I(x)$	I_0	I_0	$\left(\frac{I_0}{N}\right)^2 \left[N e^{4\sigma_\ell^2} - N^2 + 2 \sum_{i \neq j} e^{4 C_\ell(\rho_{ij})}\right]$	$\frac{I_0^2}{N} (e^{4\sigma_\ell^2} - 1)$
$I^2(x)$	$I_0^2 e^{4\sigma_\ell^2}$	$I_0^2 e^{4\sigma_\ell^2}$	$\frac{I_0^4}{N^2}\left[N e^{24\sigma_\ell^2} - N^2 e^{8\sigma_\ell^2} + 2 \sum_{i \neq j} e^{8(\sigma_\ell^2 + 2 C_\ell(\rho_{ij}))}\right]$	$\frac{I_0^4}{N} e^{8\sigma_\ell^2} (e^{16\sigma_\ell^2} - 1)$
$I^2(x_i)$	$I_0^2 e^{4\sigma_\ell^2}$	$I_0^2 e^{4\sigma_\ell^2}$	$I_0^4 e^{8\sigma_\ell^2} (e^{16\sigma_\ell^2} - 1)$	$I_0^4 e^{8\sigma_\ell^2} (e^{16\sigma_\ell^2} - 1)$
$\ln I(x_i)$	$\ln I_0 - 2\sigma_\ell^2$	$\ln I_0 - 2\sigma_\ell^2$	$4\sigma_\ell^2$	$4\sigma_\ell^2$
$\ln I^2(x_i)$	$2 \ln I_0 - 4\sigma_\ell^2$	$2 \ln I_0 - 4\sigma_\ell^2$	$16\sigma_\ell^2$	$16\sigma_\ell^2$
$\ln I(x)$	$\ln\left\{\frac{I_0}{\left[1 + \frac{1}{N^2}(N e^{4\sigma_\ell^2} - N^2 + 2 \sum_{i \neq j} e^{4 C_\ell(\rho_{ij})})\right]^{1/2}}\right\}$; $\ln\left\{\frac{I_0}{\left[1 + \frac{1}{N}(e^{4\sigma_\ell^2} - 1)\right]^{1/2}}\right\}$		$\ln\left\{1 + \frac{1}{N^2}\left[N e^{4\sigma_\ell^2} - N^2 + 2 \sum_{i \neq j} e^{4 C_\ell(\rho_{ij})}\right]\right\}$	$\ln\left[1 + \frac{1}{N}(e^{4\sigma_\ell^2} - 1)\right]$
$\ln I^2(x)$	$\ln\left\{\frac{I_0^2 e^{4\sigma_\ell^2}}{\left[1 + \frac{1}{N^2}(N e^{16\sigma_\ell^2} - N^2 + 2 \sum_{i \neq j} e^{16 C_\ell(\rho_{ij})})\right]^{1/2}}\right\}$; $\ln\left\{\frac{I_0^2 e^{4\sigma_\ell^2}}{\left[1 + \frac{1}{N}(e^{16\sigma_\ell^2} - 1)\right]^{1/2}}\right\}$		$\ln\left\{1 + \frac{1}{N^2}\left[N e^{16\sigma_\ell^2} - N^2 + 2 \sum_{i \neq j} e^{16 C_\ell(\rho_{ij})}\right]\right\}$;	$\ln\left[1 + \frac{1}{N}(e^{16\sigma_\ell^2} - 1)\right]$

$I(x_i) = I_0 e^{2\ell(x_i)}$

N = NUMBER OF DETECTORS

$I(x) = \frac{1}{N} \sum_i I_i$

$I^2(x) = \frac{1}{N} \sum_i I_i^2$

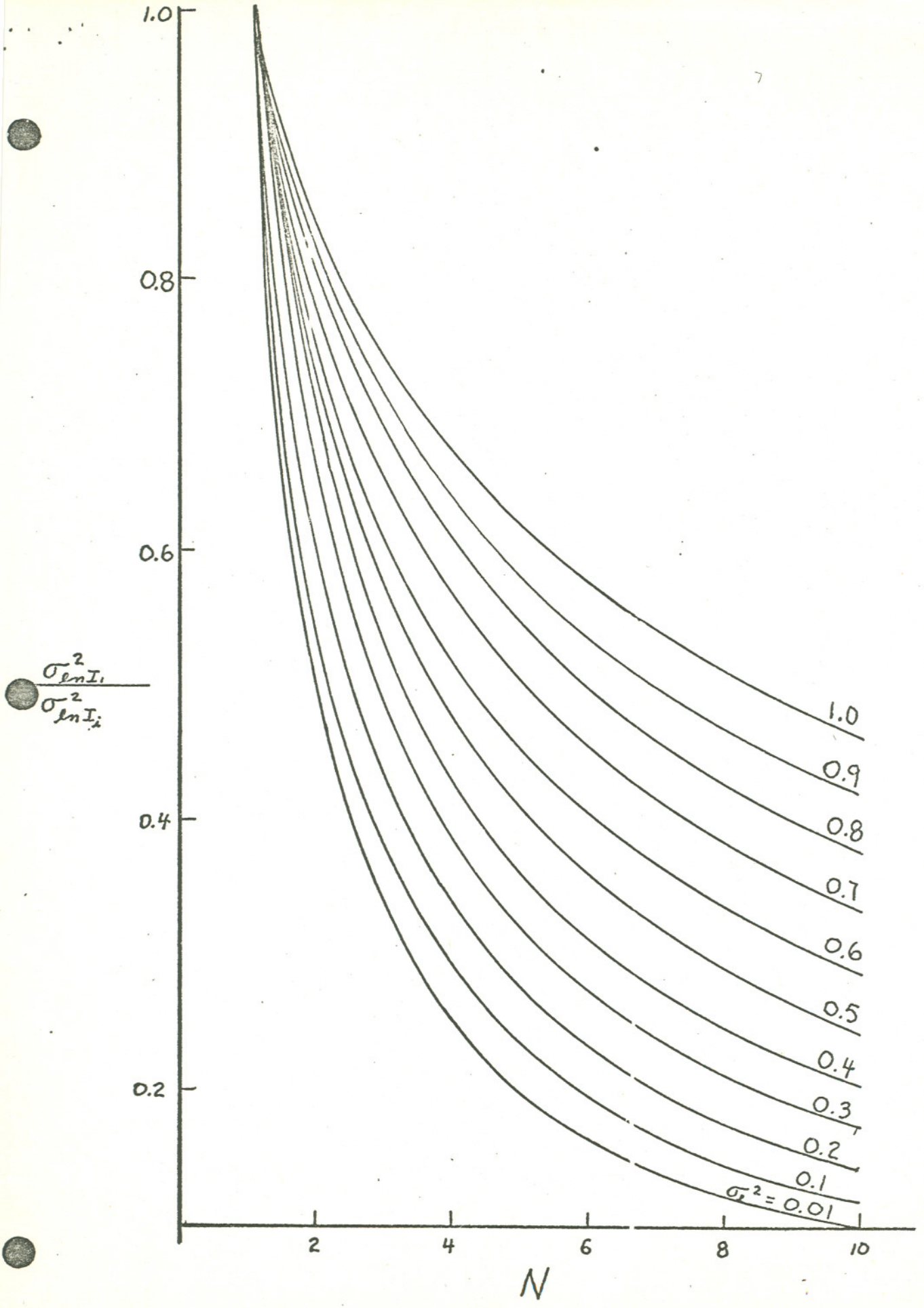

Figure 1. Normalized Log Intensity variance for the sum signal vs number of detectors with σ_ℓ^2 as a parameter.

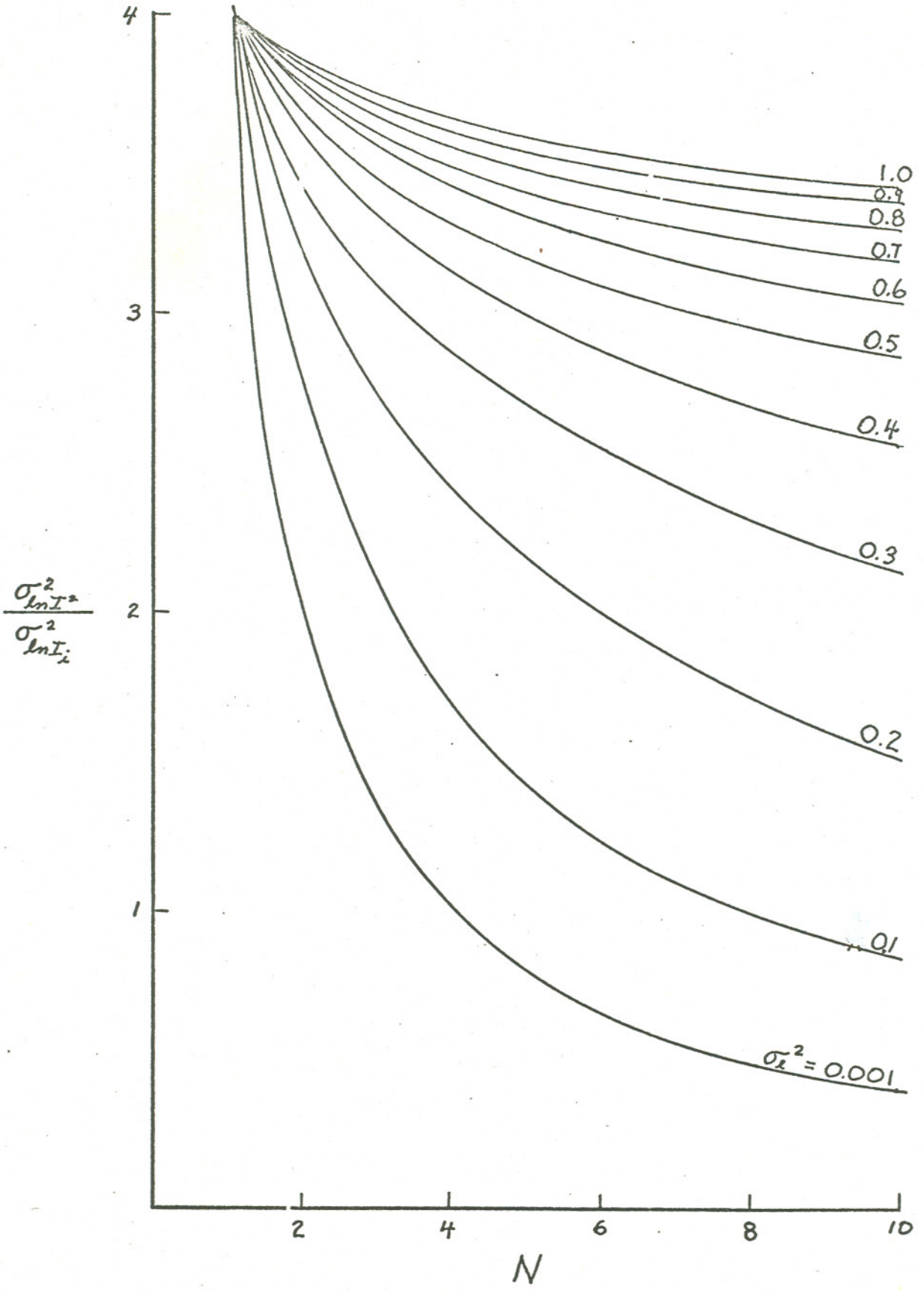

Figure 2. Normalized Log Intensity variance for the sum of squares signal vs. number of detectors, with σ_ℓ^2 as a parameter.

link is better when the signals are squared before combining. The reason for this is that because of the nonlinear weighting, the individual signals with the best signal-to-noise ratios are given the largest weight.

Note that in the analysis above, all resulting signals are assumed to be log normal. It has been shown,[14] that to a good approximation, the sum of several log normal random variables result in a random variable that is log normal. In addition note that

$$I^2(x_i) = I_o^2 \, e^{4\ell(x_i)}$$

which is also log normal. The photon bucket may be considered to be made up of N uncorrelated amplitude patches when that approximation is valid. The case of interest here, when $C_\ell(\rho_{ij}) \neq 0$ for $i \neq j$ requires numerical analysis that has not been completed.

The case of a symmetric binary communication channel in the presence of gaussian noise has been treated by Fried and Schmeltzer (Ref. 15). Their results are directly applicable to our case for both a single array element and the configuration when the individual signals are simply added. For the case of simple addition, both the log amplitude variance is reduced as shown in Fig. 1, and the signal-to-noise ratio is increased as can be seen from the following. For simple addition, it has been shown that $\eta_{I_1} = \eta_{I_i} = I_\sigma$. If, in a manner similar to that for I_1, we define a noise random variable $N = \frac{1}{N} \sum_{i=1}^{N} N_i$ where n_i represents the noise for an individual channel and is normally distributed with mean

η_{n_i} and variance $\sigma^2_{n_i}$. Then $\sigma^2_n = \frac{1}{N}\,\sigma^2_{n_i}$, and defining the signal-to-noise ratio as $\frac{\eta}{\sigma}$, then the signal-to-noise ratio for a single detector is

$$\left(\frac{S}{N}\right)_i = \frac{\eta_{I_i}}{\sigma_{n_i}} = \frac{I_o}{\sigma_{n_i}}$$

while that for the sum is:

$$\left(\frac{S}{N}\right)_1 = \frac{\eta_{I_1}}{\sigma_n} = \frac{I_o}{\sigma_{n_i}/\sqrt{N}} = \sqrt{N}\left(\frac{S}{N}\right)_i$$

Thus, the signal-to-noise ratio has been improved by $\sqrt{N}$. Hence for simple addition, we see an improvement in performance both due to an increase in the signal-to-noise ratio, and a decrease in the log amplitude variance.

The case of non-linear weighting is not so straightforward since the noise in the resulting signal is no longer gaussian. It is worthwhile to point out, however, that while the log amplitude variance may or may not be decreased over that of a single detector (depending on the number of elements in the array, and σ^2_ℓ) the signal-to-noise ratio is always improved, the increase being greatest in cases of high turbulence. In Appendix II it is shown that on an instantaneous basis, the signal-to-noise ratio of the resultant signal is equal to the sum of the signal-to-noise ratios of the elemental signals.

The bit-error-rate of symmetric binary communications can be expressed as follows:[11,13]

$$P_E = \int_0^\infty \rho(I)\, \Phi_i(I)\, dI$$

$$\rho(I) = \frac{1}{\sqrt{2\pi\sigma^2}} \frac{1}{I} e^{-\frac{1}{2\sigma^2}(\ln I - \eta)^2}$$

$$\Phi_1(I) = \operatorname{erf}\left(-\frac{1}{2}\frac{I}{\sigma_n}\right)$$

$$\Phi_2(I) = \operatorname{erf}\left(-\frac{1}{2}\frac{I}{\sqrt{N}\sigma_n}\right)$$

where

P_E is the bit-error-rate

$P(I)$ is the probability distribution of signal at receiver

$\Phi_i(I)$ is the probability distribution of signal and noise at receiver

I is the signal level

σ^2 is the variance of signal level

η is the mean of signal level

σ_n is the RMS of noise level

N is the number of detectors

$\Phi_1(I)$ is applied to single detector and weighted sum

$\Phi_2(I)$ is applied to simple sum

As an example when $\sigma_\ell^2 = 0.1$, $I_o = 1$, $N = 4$, $\sigma_N = 1$ this bit-error-rate will be the area under the multiplication of the suitable curves in Fig. 3.

$$P(I) = \frac{1}{\sqrt{2\pi\sigma^2}} \frac{1}{I} e^{-\frac{1}{2\sigma^2}(\ln I - \mu)^2}$$

Curve (1): Single detector
Curve (2): Simple sum
Curve (3): Weighted sum
Curve (4): $\Phi_1(I) = \text{erf}\left(-\frac{1}{2}\frac{s}{\sigma_n}\right)$
Curve (5): $\Phi_2(I) = \text{erf}\left(-\frac{1}{2}\frac{s}{\sqrt{N}\sigma_n}\right)$

$\sigma_e^2 = 0.1$, $I_0 = 1$, $N = 4$, $\sigma_n = 1$

$$P_E = \int_0^\infty P(I)\,\Phi_i(I)\,dI$$

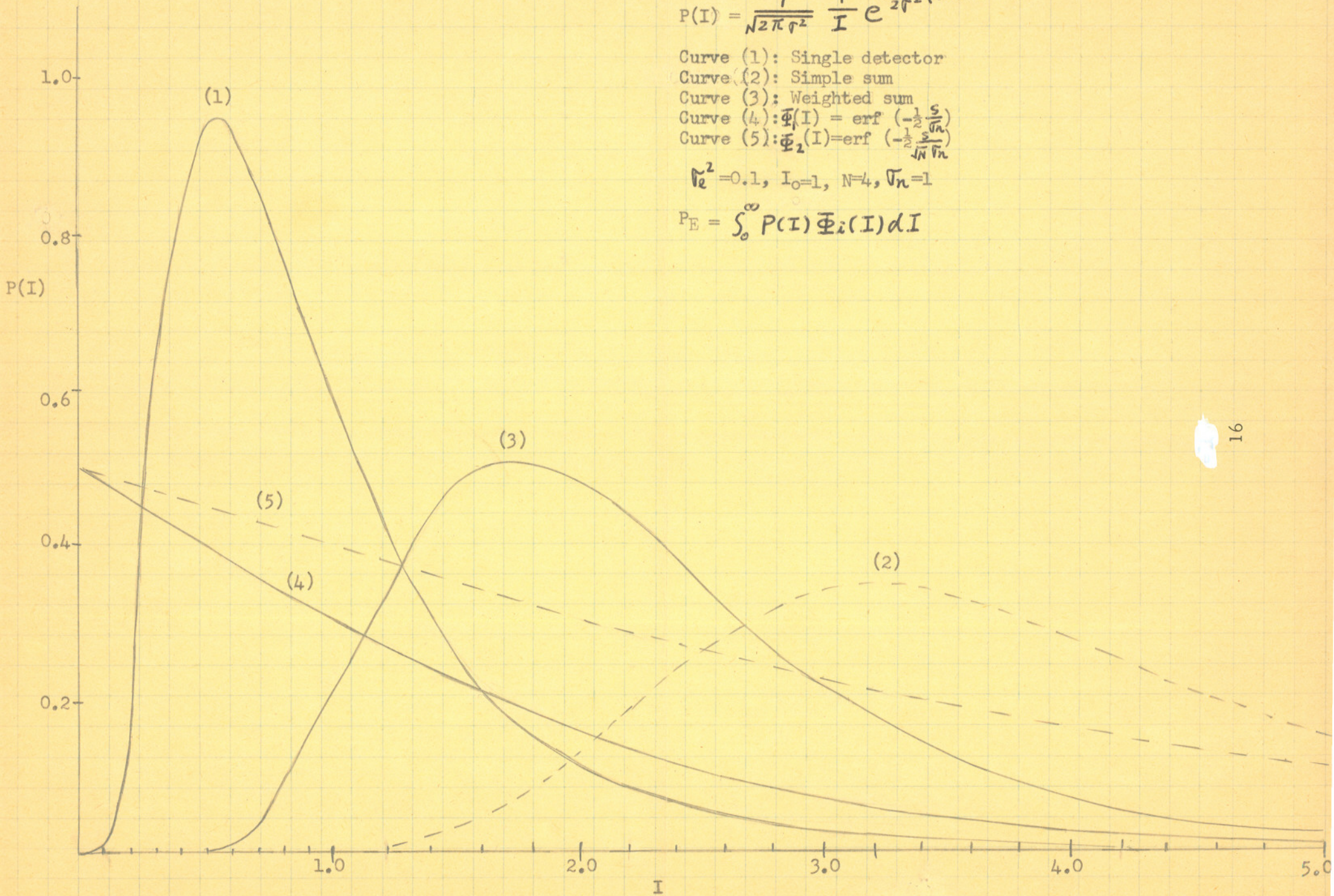

Figure 3.

III. EXPERIMENTAL PROCEDURES

An array of four, separated receivers with spacing that is variable to ensure independence of fading has been used. A photon bucket with a 20 cm diameter aperture has also been set up to compare with the performance of the array as a function of signal to noise ratio and strength of turbulence.

The experimental arrangement provides for both simple addition of the individual signals and squaring of the individual signals before addition.

The physical experiment (Fig. 4) consists of an argon laser transmitter operating at 4880Å and the three receivers described above. The transmitter (Fig. 5) is focused through a chopper to encode the binary information and then diverged toward the receiver. The chopper is a rotating wheel with slots chosen to give a 4.5 kHz pulse train with a duty cycle of 1/4. The transmitted signal is then considered to be a 9 kHz binary signal consisting of alternating ones and zeroes. Neutral density filters are provided for varying the signal level.

As described previously, the receiver end of the 1.6 kilometer path contains three separate receivers, a photon bucket (Fig. 6), an array with electronic processing (Fig. 7), and an array with optical processing (Fig. 8). Each configuration uses common decision-making electronics.

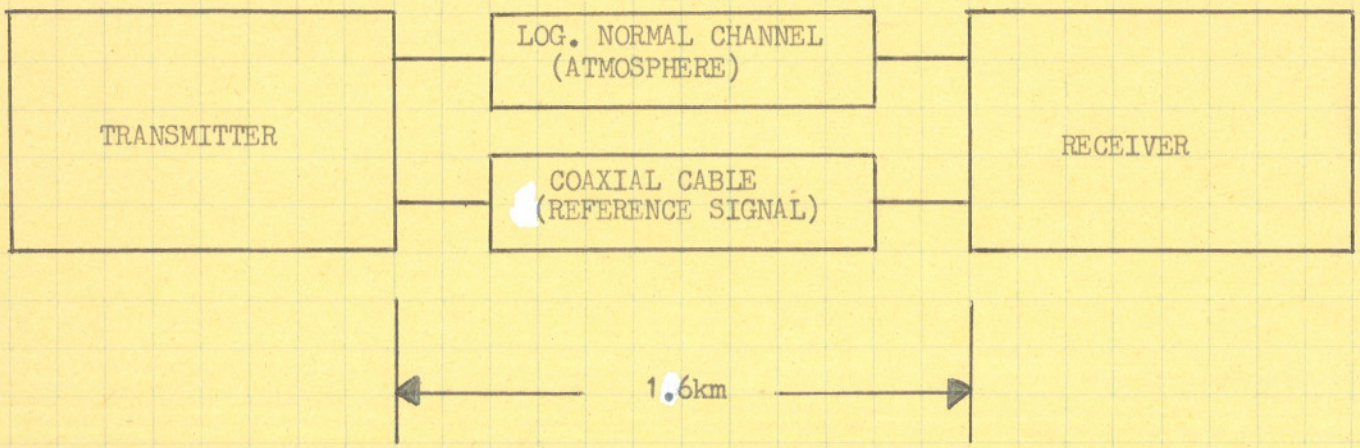

Figure 4. Block diagram for experimental set up

Beam waste at output of laser = 7×10^{-2} cm

Beam waste at chopping wheel = 2.34×10^{-3} cm

Beam waste at (9) = 3×10^{-3} cm

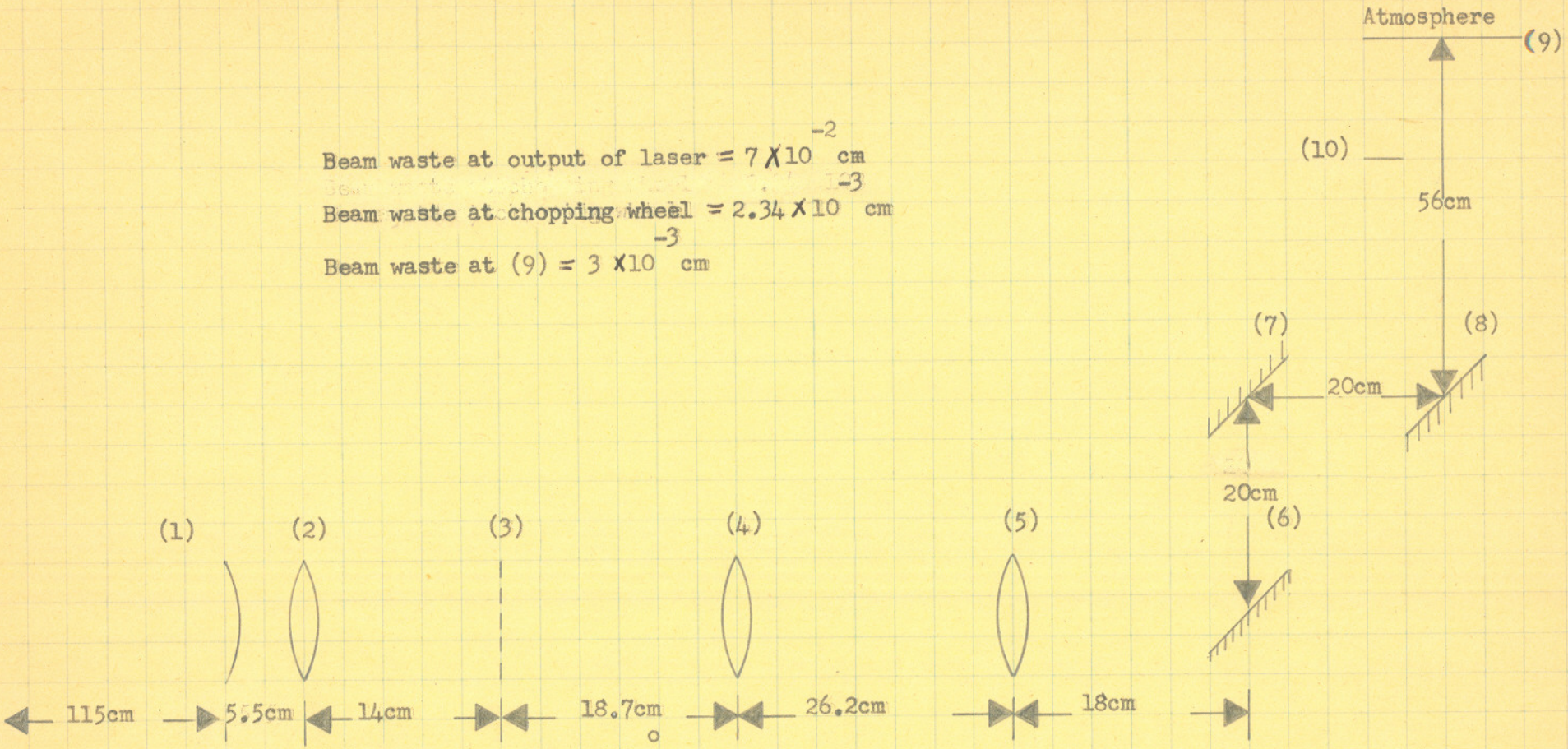

(1) Argon laser, λ = 4880 Å
(2) Lens, Focal Length= 10cm Transmission ~ 92%
(3) Chopping wheel
(4) Lens, Focal Length= 10cm Transmission ~ 92%
(5) Lens, Focal Length= 5cm Transmission ~ 92%
(6),(7),(8) Mirror
(9) Window (with variable neutral density filters plug in)
(10) Detector for reference signal

Figure 5. Optical set up for transmitter

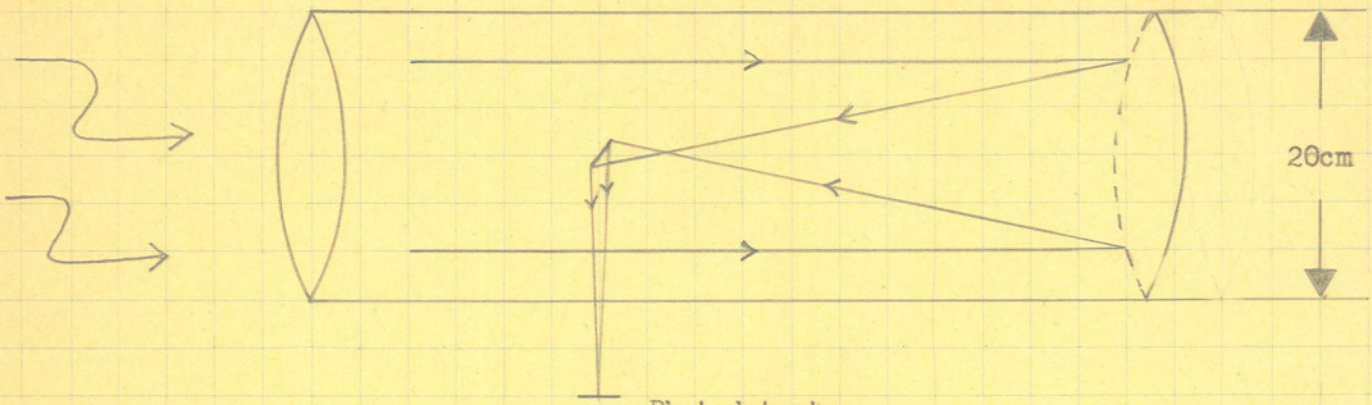

Figure 6. Photon bucket

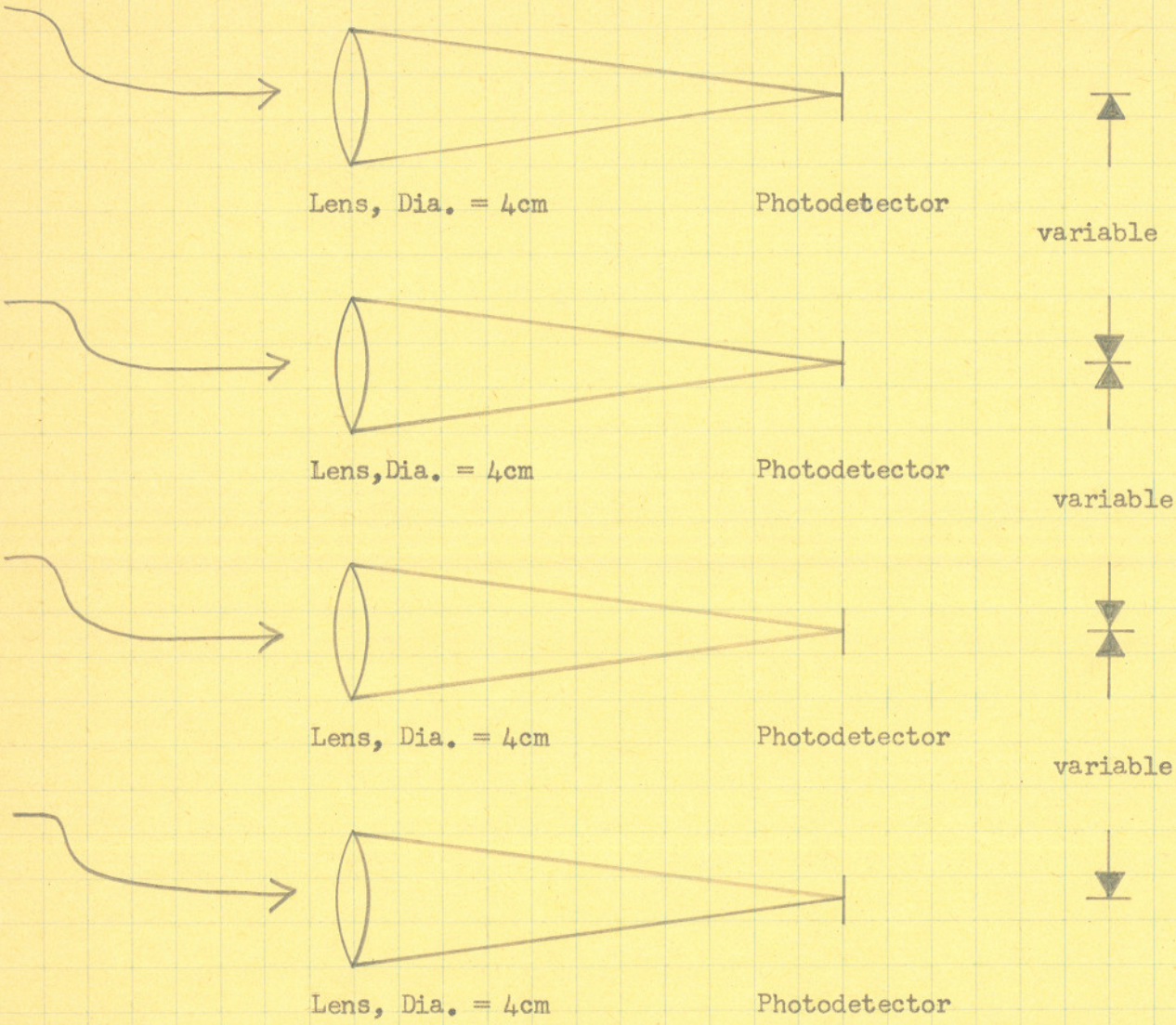

Figure 7. Array of detectors with electronic processing

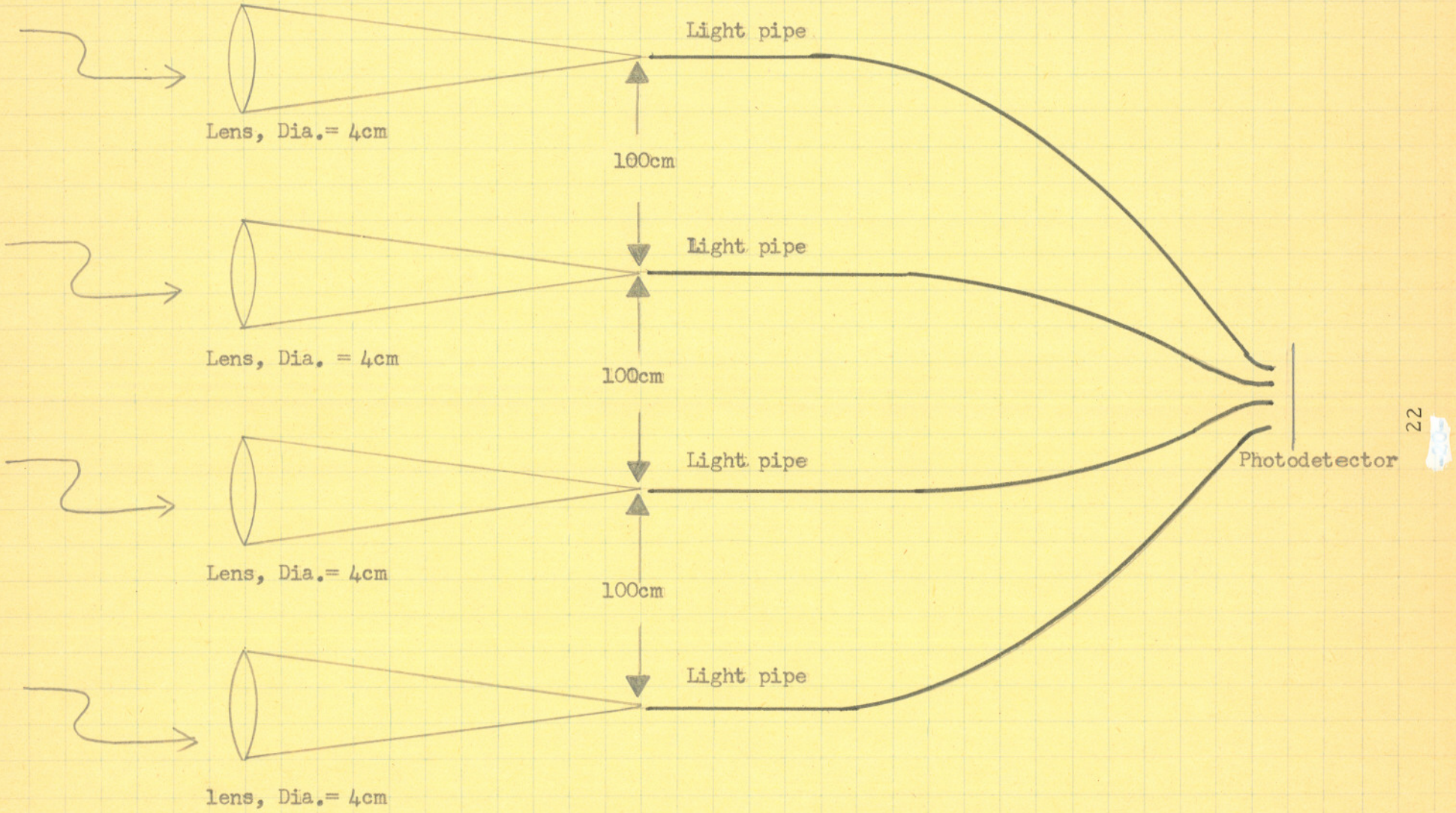

Figure 8. Array of detectors with optical processing

The photon bucket consists of a 20 cm diameter Neutonian telescope focused onto a doped silicon photodetector. The preamplifier portion of the circuit is a-c coupled to eliminate d-c effects (e.g., drift and offset). Subsequently, the signal is d.c. restored and coupled through a selector switch to the decision-making electronics.

The array with optical processing consists of four elements spaced approximately 1 meter apart. Each element consists of a 4 cm diameter lens focused onto a fiber optics bundle. The bundle from each element is brought to a common photodetector. The signal from three kinds of receivers then alternately passes through an a-c coupled pre-amplifier and is d-c restored. At this point two options are provided by means of a switch. The first option consists of simple adding the signals directly (as in the case of the optical processing) and coupling them through the selector switch to the decision-making electronics. The second option consists of the nonlinear weighting. The signal in each channel is passed through a low pass filter (3 db point is 500 Hz) to extract the component due to scintillation. This component is then fed into a multiplier along with the original signal to weight the signal in proportion to the scintillation. Following this, the signals are added together and coupled to the decision-making electronics through the selector switch.

The decision-making electronics compares the received signal with an adaptive threshold that is equal instantaneously to $\overline{S}/2$ as discussed in Appendix II where S is the received signal strength. The threshold is obtained by passing the signal through a low pass filter (3 db at 500 Hz) to obtain the average value of the signal. The received signal is integrated over the duration of a bit and then compared to the threshold. A decision is made that a "1" (or "0") occurred during the interval if the signal is greater (less) than the threshold.

In order to determine if an error (when "1" is transmitted and "0" is received) was made, the receiver decision is compared to a reference that is derived at the transmitter and hard-wired to a receiver. The output of this comparison is connected to counters. A distinction is made between errors and false alarms (when "0" is transmitted and "1" is received) and both are counted. Fig. 9 is a block diagram of the receiver and Fig. 10-1 – Fig. 10-12 are schematic diagrams and photographs of some of the oscilloscope recordings.

In addition to the above, the output signal from the three receivers and from any one of the four electronic channels (before and after non-linear weighting) is available for further processing and analysis. Any one or more of these signals may be passed through a 1 kHz bandpass filter centered at 9 kHz to extract the scintillation components on a 9 kHz carrier. This output is then demodulated and passes through a

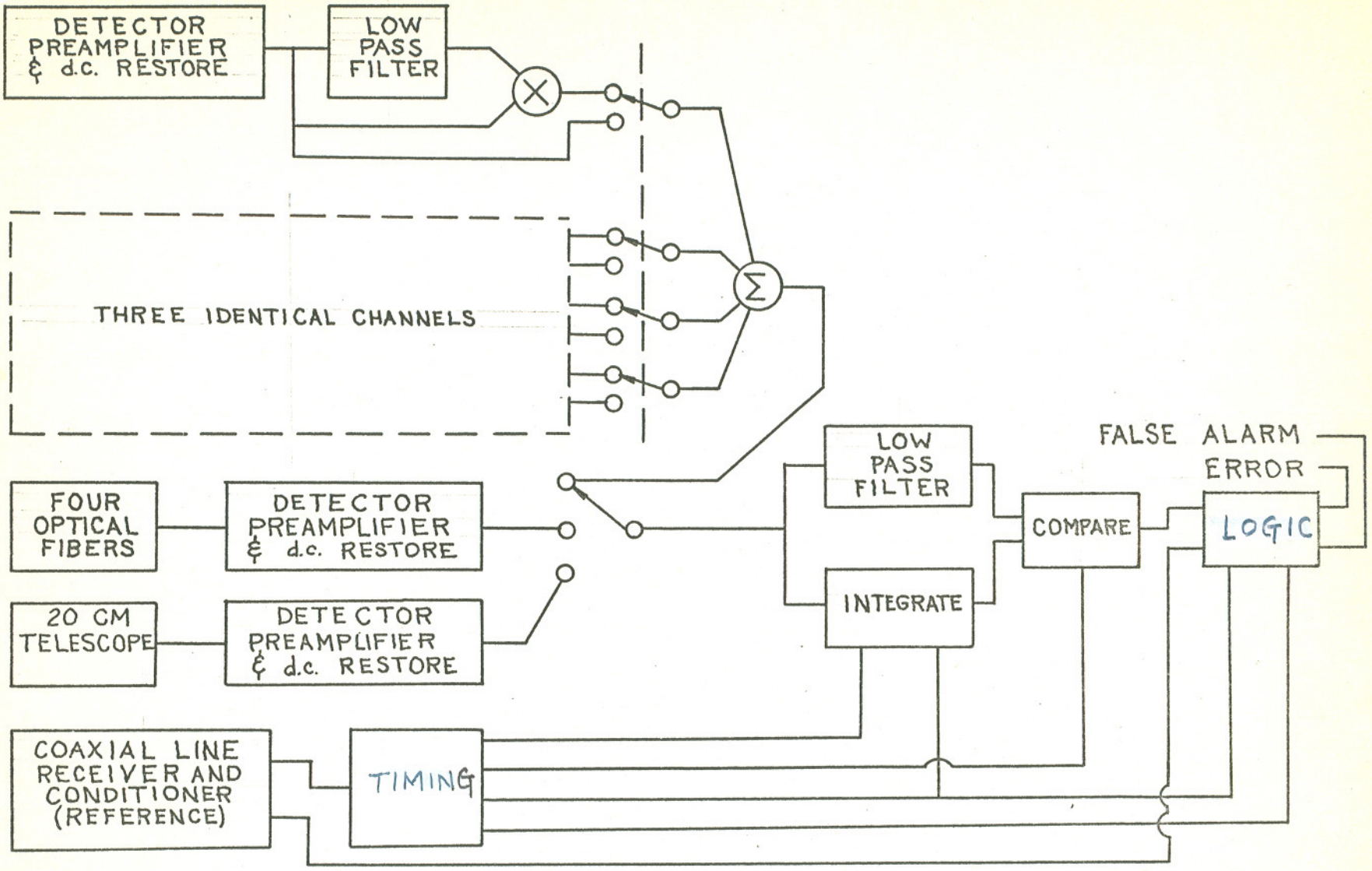

Figure 9. Block Diagram of Direct Detection Diversity Receiver.

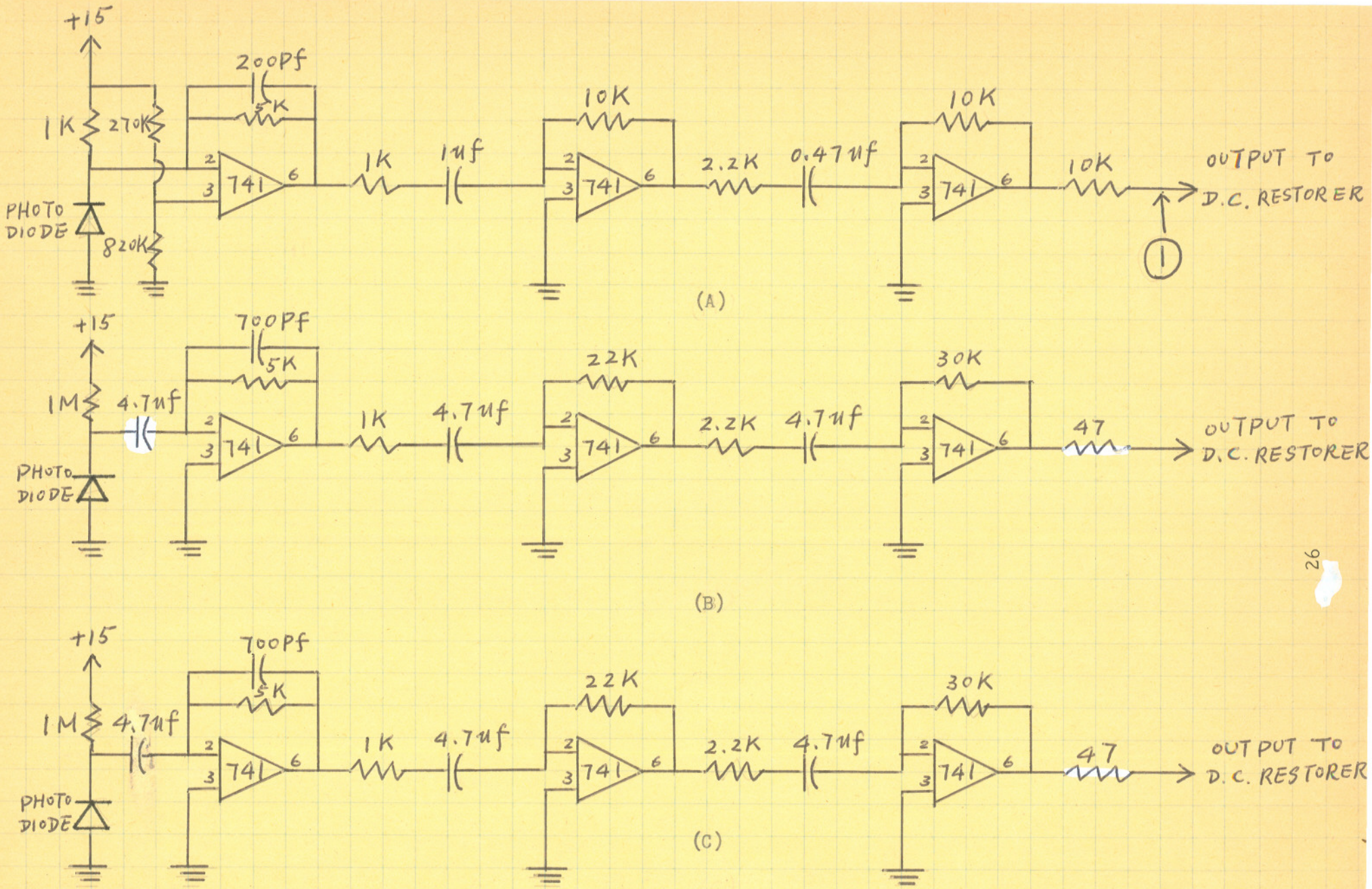

Figure 10-1 (A) Electronic processing detector and preamplifier
(B) Photon bucket detector and preamplifier
(C) Optical processing detector and preamplifier

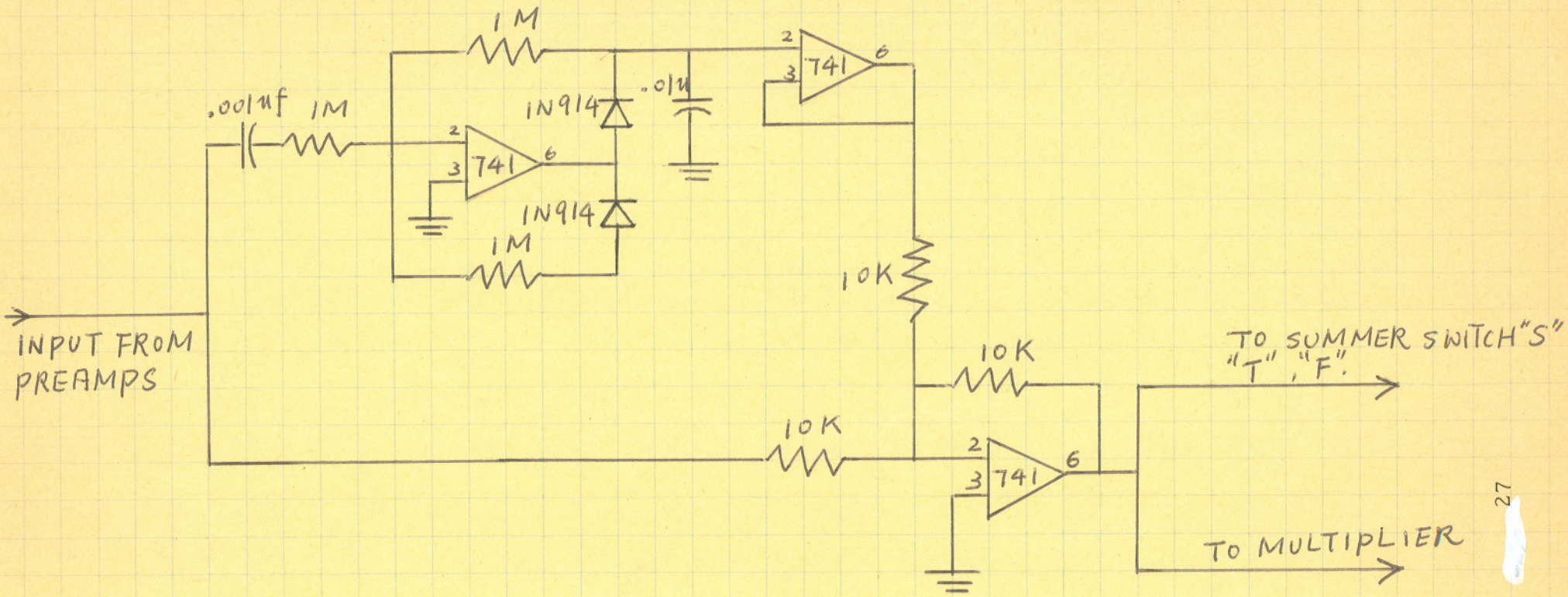

Figure 10 - 2. D. C. restorer for three kind receivers

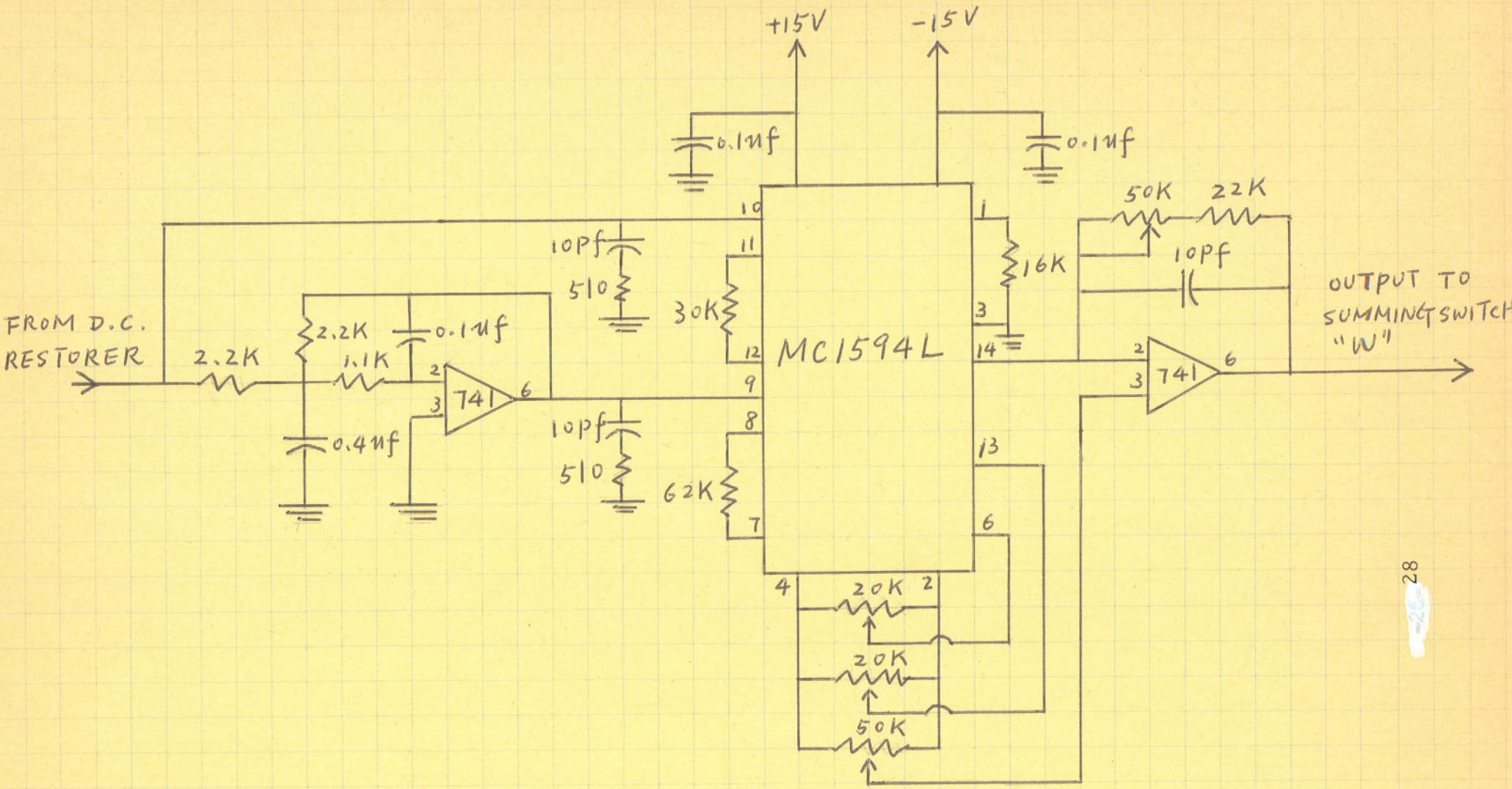

Figure 10-3. Low pass filter and multiplier

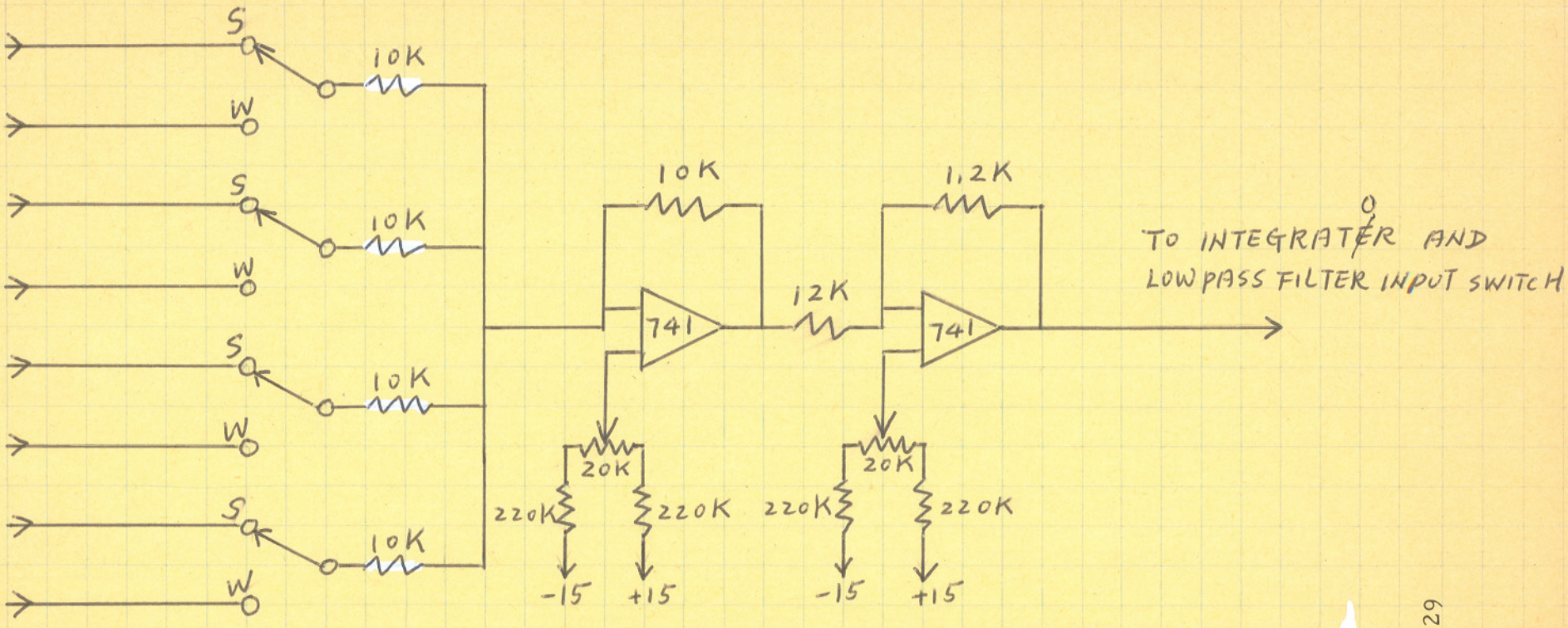

Figure 10-4. Summing amplifier

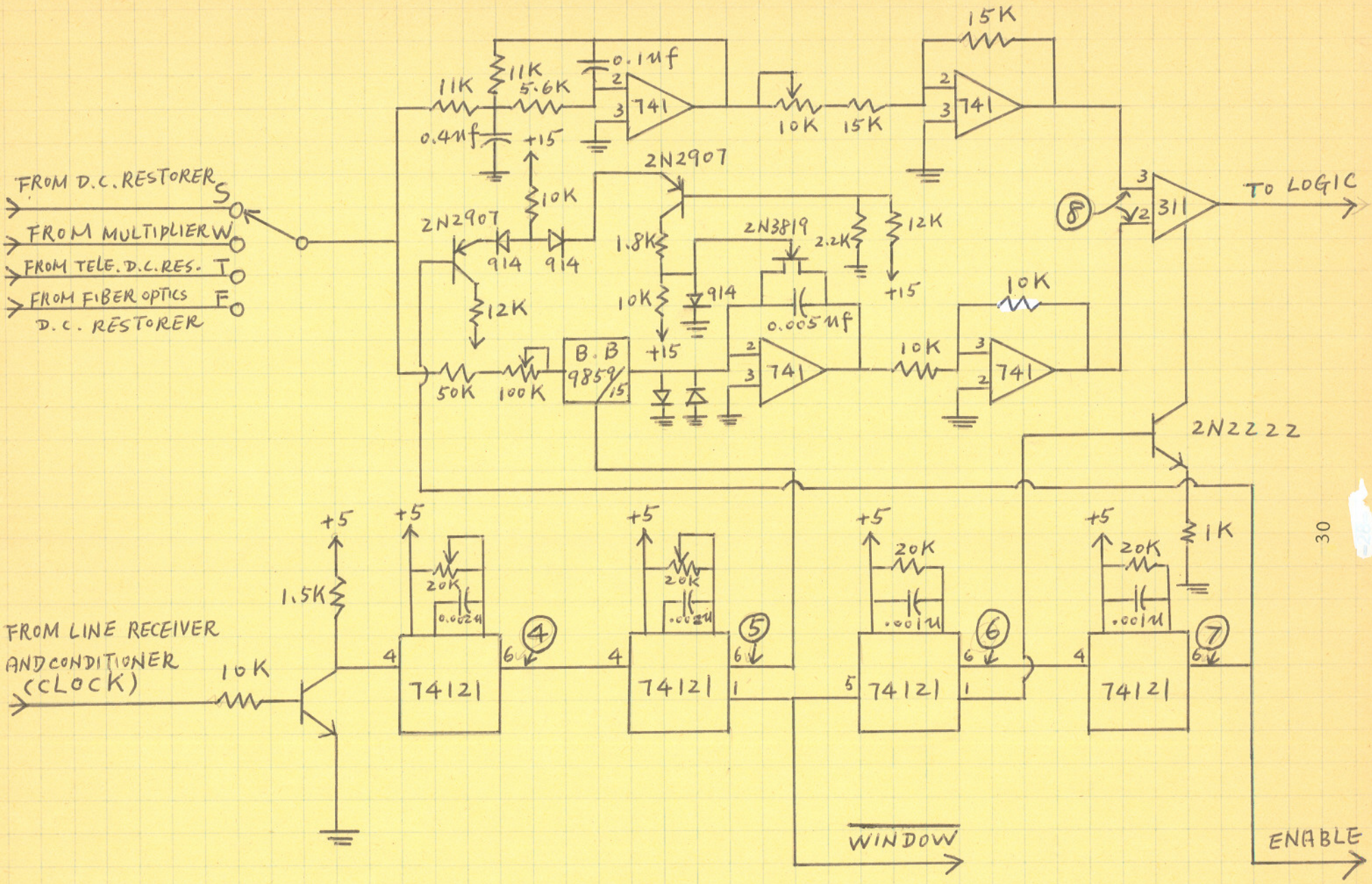

Figure 10-5. Low pass filter, integrator, timing circuit and comparator

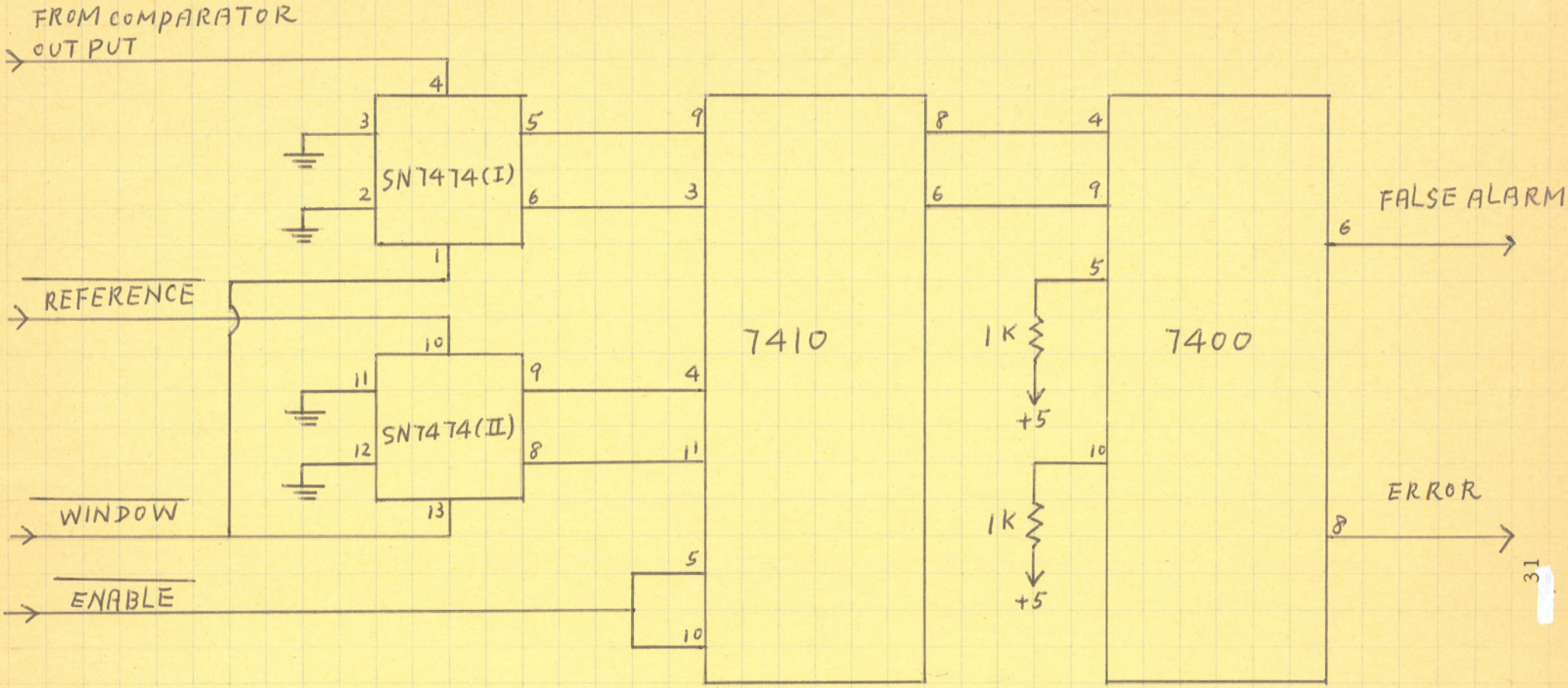

Figure 10-6 Logic circuit

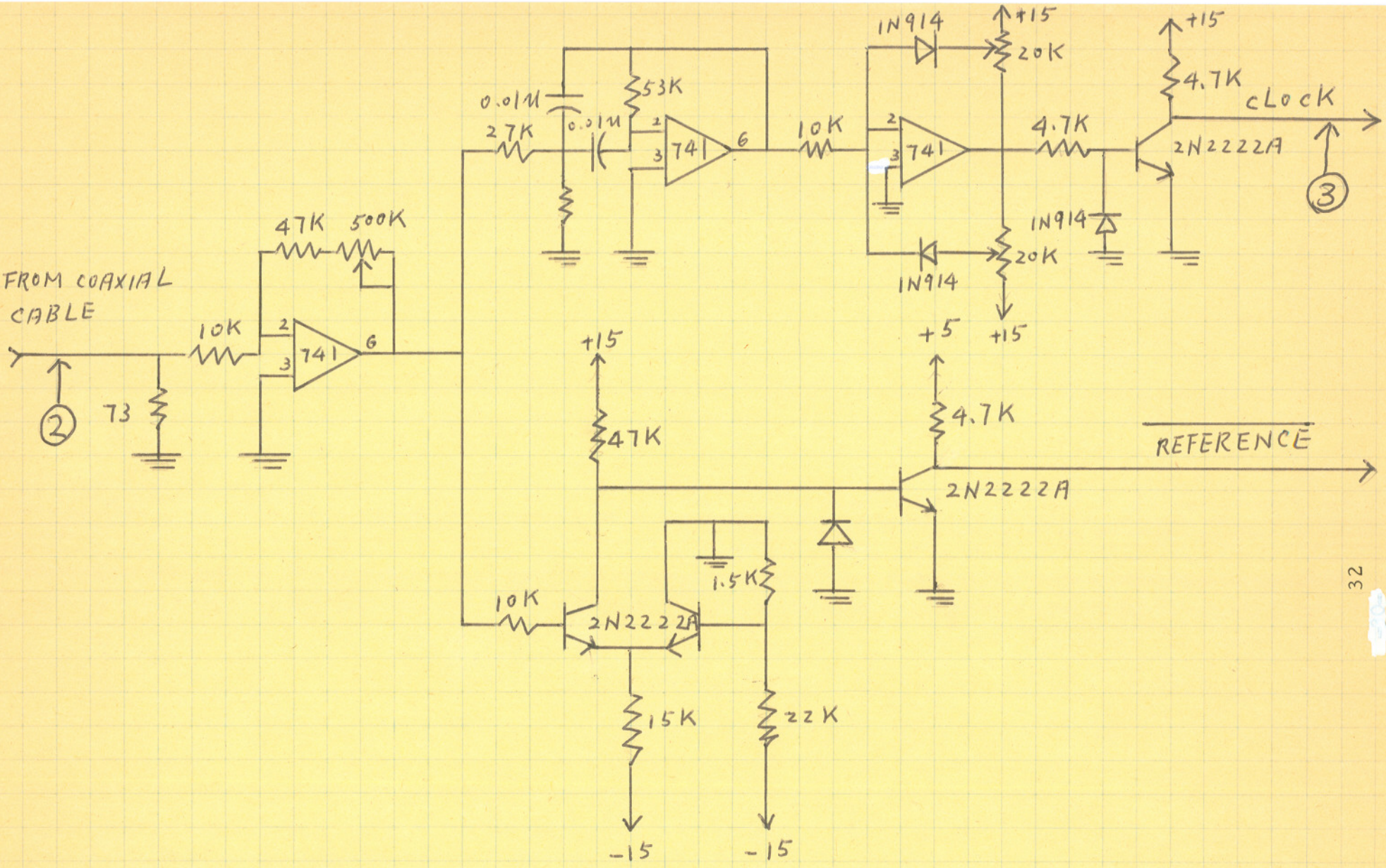

Figure 10-7. Line receiver and conditioner

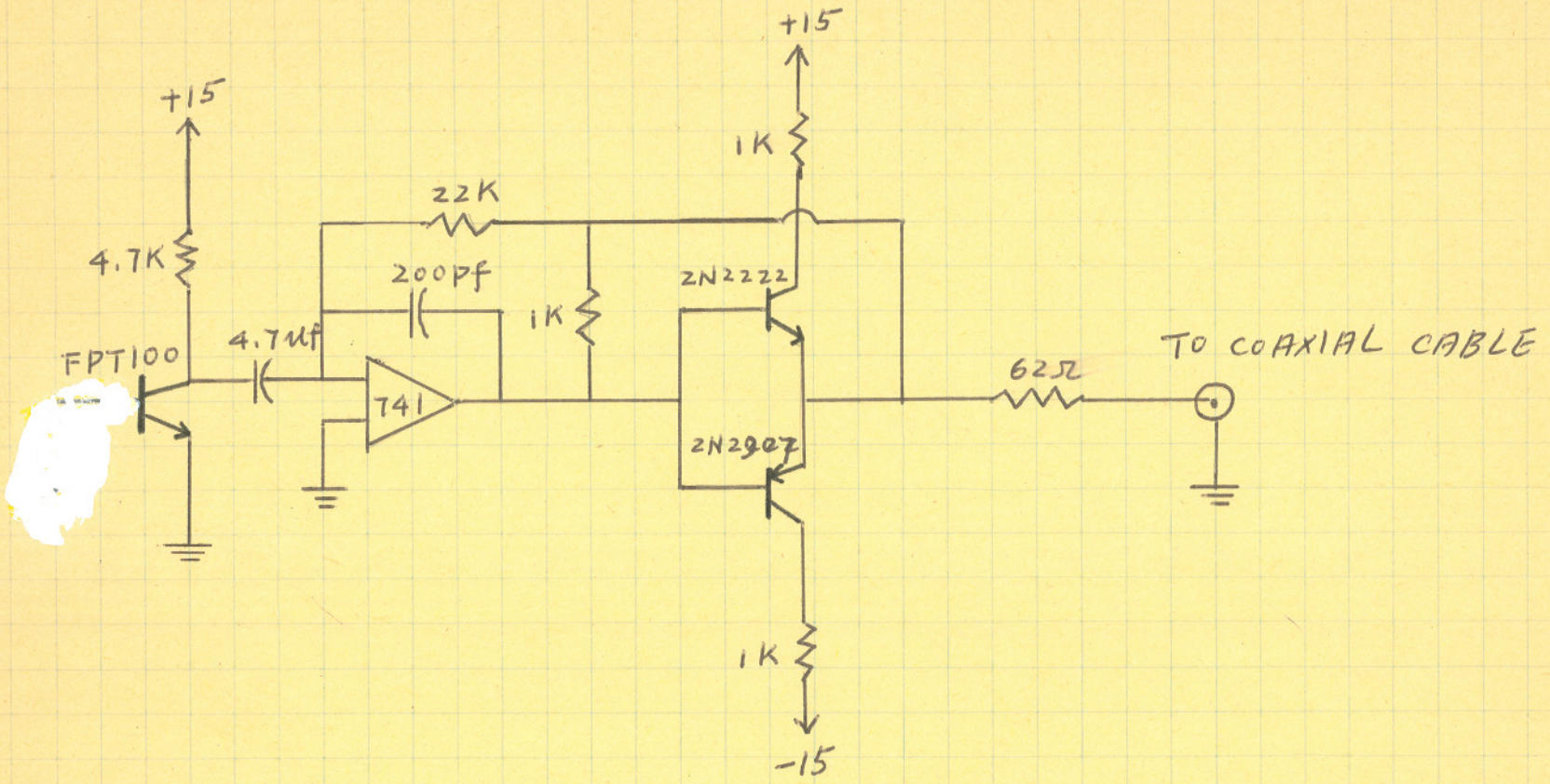

Figure 10-8. Reference transmitter

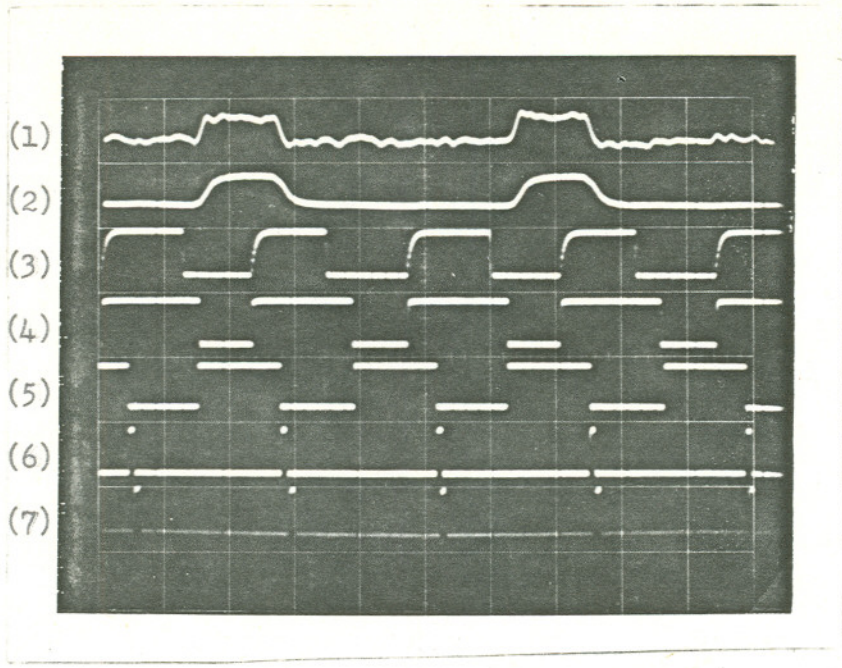

Figure 10-9. Wave form at points (1),(2),(3),(4),(5) (6),(7) on schematic

	Ver. V/cm	Hori. μs/cm
(1) Signal from one detector	0.5	50
(2) Reference signal	2	50
(3) Clock Signal	20	50
(4) First one shot output	5	50
(5) Second one shot output	5	50
(6) Third one shot output	5	50
(7) Fourth one shot output	5	50

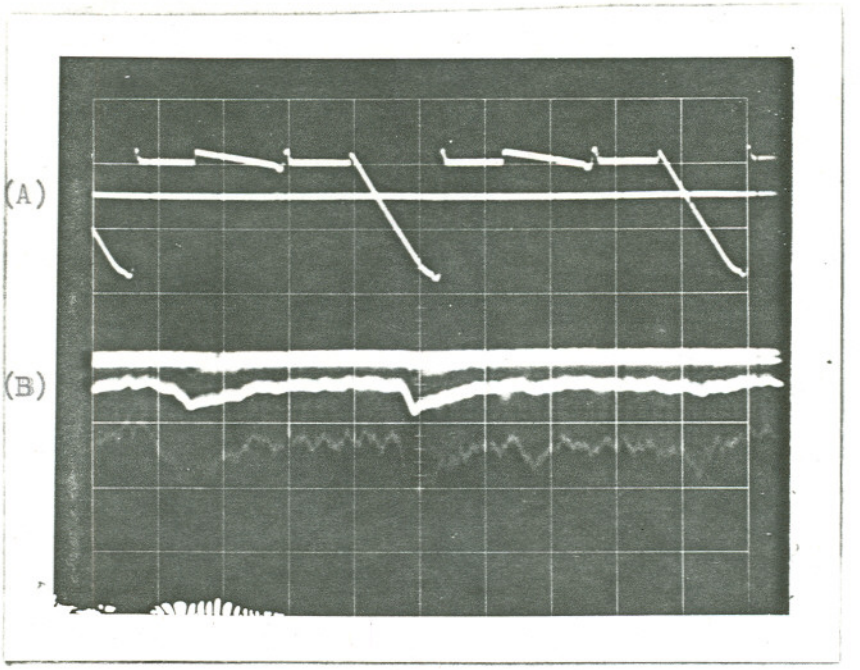

Figure 10-10. Wave form of integrator output and threshold level at different scales (i,e,) Wave form at point (8) on schematic

(A) Ver. 0.5 v/cm, Hori. 50 μs/cm

(B) Ver. 0.5 v/cm, Hori. 10 ms/cm

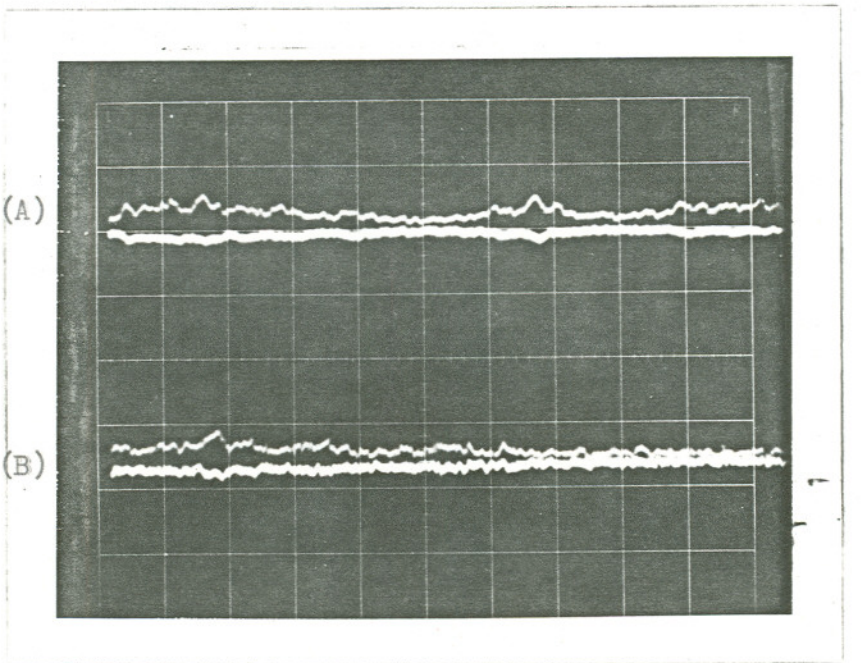

Figure 10 - 11. Simple add sum output and weighted add sum output

(A) Simple add sum output Ver. 0.5 v/cm, Hori. 10 ms/cm

(B) Weighted add sum output Ver. 0.5 v/cm, Hori. 10 ms/cm

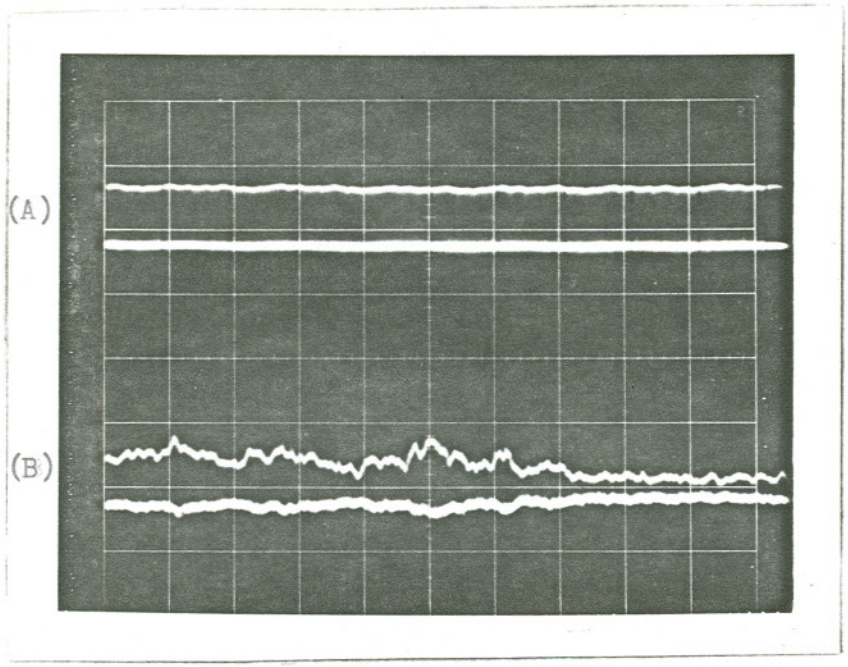

Figure 10 - 12. Reference signal and signal output from one detector

(A) Reference signal Ver. 1 v/cm, Hori. 10 ms/cm (i,e,) Wave form at point (2) on schematic
(B) Signal output from one detector Ver. 1 v/cm Hori. 10 ms/cm (i,e,) Wave form at point (1) on schematic

logarithmic amplifier where the log irradiance may be recorded on tape. Further, a point receiver at the site is available so the log irradiance of a point receiver may be simultaneously recorded. Computer programs were used[16] for processing the log irradiance data to obtain the desired statistical averages.

The noise in each channel was measured at the output of each three stage preamplifier, and after electronic processing by an RMS meter.

Finally, C_n^2 [5,6] was recorded using in-house equipment that has been previously described,[8] along with meterological parameters such as temperature, pressure, wind velocity and direction, and humidity.

IV. RESULTS

Table 2 through Table 6 show some preliminary data taken during July and August 1974, where

σ_{Pt}^2 = Variance of point detector

σ_1^2 = Variance of one detector

$\sigma_2^2(S)$ = Variance of two detectors simple addition

$\sigma_2^2(W)$ = Variance of two detectors weighted addition

$\sigma_3^2(S)$ = Variance of three detectors simple addition

$\sigma_3^2(W)$ = Variance of three detectors weighted addition

$\sigma_4^2(S)$ = Variance of four detectors simple addition

$\sigma_4^2(W)$ = Variance of four detectors weighted addition

The data, in the simple addition case shows quite a good fit to the theoretical prediction; in the weighted case, there is not as good a fit to the theoretical prediction. The reason may be that not enough data was collected to show the statistical properties.

The data for the bit-error-rate is still being collected. Unfortunately, no quantitative data analysis is available at this time.

TABLE 2

Date:	7-23-74 afternoon
Separation of array elements:	40.6 cm
Temperature:	24.5°C
Humidity:	36
Wind Speed:	2.24 m/sec
Wind Direction:	north
Atmospheric Pressure:	30.2 in.
Cn^2:	$7.57 \times 10\text{-}12\ m^{-2/3}$

σ^2_{Pt}	σ_1^2	$\sigma_2^2(S)$		$\sigma_3^2(S)$		$\sigma_4^2(S)$	
		Exp.	The.	Exp.	The.	Exp.	The
0.150	0.105						
0.160	0.106	0.0435	0.054				
0.042	0.121			0.039	0.042		
0.154	0.570						
0.163	0.124					0.003	0.032

TABLE 3

Date:	7-24-74 afternoon
Separation of array elements	40.6 cm
Temperature:	28° C
Humidity:	35
Wind Speed:	2.91 m/sec
Wind Direction:	east
Atmospheric press.:	30.2 in.
Cn^2:	$5.16 \times 10^{-12} m^{-2/3}$

TABLE 3(A)

Sep	σ^2_{Pt}	σ_1^2	σ_2^2(S)		σ_3^2(S)	
			Exp.	The.	Exp.	The.
1'4"	0.169	0.115	0.059	0.059		
1'4"	0.168	0.118			0.044	0.041
2'8"	0.192	0.137			0.056	0.048

TABLE 3(B)

Sep	$\sigma^2_{Pt.}$	σ_1^2	σ_2^2(W)		σ_3^2(W)	
			Exp.	The.	Exp.	The.
1'4"	0.178	0.120	0.267	0.269		
1'4"	0.173	0.125			0.159	0.196
2'8"	0.182	0.123	0.360	0.276		

TABLE 4

Date:	7-31-74 afternoon
Separation of array elements:	40.6 cm
Temperature:	34.5°C
Humidity:	35
Wind Speed:	3.58 m/sec
Wind Direction:	north
Atmospheric pressure:	30 in.
Cn^2 :	$6.573 \times 10^{-12} m^{-2/3}$

TABLE 4(A)

σ_1^2	σ_2^2(S)		σ_3^2(S)		σ_4^2(S)	
	Exp.	The.	Exp.	The.	Exp.	The.
0.127	0.0807	0.066				
0.178			0.0843	0.0629		
0.144					0.0429	0.038

TABLE 4(B)

σ_1^2	σ_2^2(W)		σ_3^2(W)		σ_4^2(W)	
	Exp.	The.	Exp.	The.	Exp.	The.
0.142	0.206	0.324				
0.129			0.0854	0.203		
0.163					0.145	0.206

TABLE 5

Date:	8-2-74 afternoon
Separation of array elements:	40.6 cm
Temperature:	32.8°C
Humidity:	35
Wind Speed:	3.35 m/sec
Wind Direction:	north
Atmospheric Press.	-
Cn^2 :	-

σ^2_{Pt}	σ_1^2	σ_4^2(S)		σ_4^2(W)	
		Exp.	The.	Exp.	The.
0.317	0.070	0.062	0.018		
0.299	0.066			0.0937	0.073

TABLE 6

Date:	8-5-74 afternoon
Separation of array elements:	40.6 cm
Temperature:	29.3°C
Humidity:	33
Wind Speed:	0.89 m/sec
Wind direction:	west
Atmospheric pressure:	30 in.
Cn^2:	$7.484 \times 10^{-13} m^{-2/3}$

σ_1^2	$\sigma_3^2(S)$		$\sigma_4^2(S)$	
	Exp.	The	Exp.	The.
0.13 0.14	0.046	0.045	0.02	0.036

$Cn^2 = 5.35 \times 10^{-13} m^{-2/3}$

σ_{Pt}^2	σ_1^2	$\sigma_2^2(S)$	
		Exp.	The.
0.33	0.18	0.091	0.094

V. DISCUSSION

The primary objective of this program was to demonstrate how to overcome amplitude scintillation in a practical direct direction receiver. Previous experimental work showed that under conditions of saturation, the received field exhibits a significant correlation over large distances (~ tens of centimeters). This suggested that in order to obtain maximum advantage of "aperture averaging" that the receiver must have:

1. An extremely large aperture, or
2. Consist of several apertures spaced at large distances.

The object of this project was to design, build and test a system that could be used to experimentally demonstrate the advantage of a receiver as described in (2) over one consisting of a single aperture with a similar area.

Theoretical considerations were given in Section II. These indicated that the amplitude fading (db) of a received signal can be decreased approximately by a factor N (number of detectors) and the signal to noise ratio can be increased by a factor $\sqrt{N}$ by using N independent detectors followed by electronic addition. The signal to noise ratio of a communication link can be further improved by squaring (nonlinear weight) the photo current from the detectors, and then adding them together. However, the nonlinear weighting increases the log

amplitude variance, so that even though the resulting signal fading decreases as a function of the number of detectors, it is always larger than in the simple addition case. The bit-error- rate of a symmetric binary communication channel is better in the weighted addition case than in the simple addition case as analysed in Figure (3).

The receiver design was described in Section III. The unique features of the receiver are:

1. Multiple, variable spacing apertures.
2. Weighted addition.
3. Adaptive threshold.

Testing of the receiver gave the preliminary data given in Section IV. This data agrees with the theory as shown in Table 2 through Table 6.

The equipment is being used in a continuing experimental program that will result in a quantitative comparison of the different receiver configurations. It is expected that the multiple aperture receiver will offer a significant performance advantage over the photon bucket.

The primary contribution of this work was the analysis and fabrication of an experimental optical communication receiver that can be used to quantify the effects of the atmosphere on an optical cummunication

system and the optimum receiver for optical communication through the atmosphere. Finally, the electronics developed in this program will be used not only in the direct detection system described here, but in conjunction with an optical heterodyne receiver that is under development.

Appendix I

Statistical Averages

Note that if $y = e^{x}$ where x is a normally distributed random variable with mean and variance η_x and σ_x^2 respectively, then[11]

$$\eta_y = \langle y \rangle = e^{\eta_x + \frac{\sigma_x^2}{2}}, \text{ and} \tag{1}$$

$$\sigma_y^2 = \langle (y - \langle y \rangle)^2 \rangle$$

$$= e^{2\eta_x + \sigma_x^2} (e^{\sigma_x^2} - 1)$$

$$= \eta_y^2 (e^{\sigma_x^2} - 1) \tag{2}$$

These expressions are useful in finding statistical averages of log normal random variables, e.g., y above.

Consider the received irradiance

$$I(x_i) = I_o e^{2\ell(x_i)}$$

= irradiance at a point x_i, where $\ell(x_i)$ is a normally distributed random variable with mean η_ℓ and variance σ_ℓ^2. Then from (1)

$$\langle I(x_i) \rangle = I_o \langle e^{2\ell(x_i)} \rangle$$

$$= I_o e^{2\eta_\ell + 2\sigma_\ell^2}$$

If I_o is the average value of the irradiance with no scintillation present, then the average value of irradiance in the presence of scintillation must be I_o due to conservation of energy.[11] Therefore

$$\langle e^{2\ell(x_i)} \rangle = e^{2\eta_\ell + 2\sigma_\ell^2} = 1$$

$$\text{and } \eta_\ell = -\sigma_\ell^2 \tag{3}$$

Using this,

$$\sigma_{I_i}^2 = \langle [I(x_i) - \langle I(x_i) \rangle]^2 \rangle$$

$$= \langle I^2(x_i) \rangle - I_o^2$$

$$= \langle I_o^2 \, e^{4 \ell(x_i)} \rangle - I_o^2$$

$$= I_o^2 \, [\langle e^{4 \ell(x_i)} \rangle - 1]$$

From (1) and (3),

$$\langle e^{4 \ell(x_i)} \rangle = e^{4 \eta_\ell + 8 \sigma_\ell^2}$$

$$= e^{4 \sigma_\ell^2}$$

and $\sigma_{I_i}^2 = I_o^2 \, (e^{4 \sigma_\ell^2} - 1)$

Now consider the random variable

$$I_1(x) = \frac{1}{N} \sum_{i=1}^{N} I(x_i)$$

as in the text. To carry out the formal computation of the variance in more detail;

$$\sigma_{I_1}^2 = \left\langle \left(\frac{1}{N} \sum_i I(x_i) - \left\langle \frac{1}{N} \sum_i I(x_i) \right\rangle \right)^2 \right\rangle$$

$$= \left(\frac{I_o}{N} \right)^2 \Big\langle \sum_i \sum_j e^{2[\ell(x_i) + \ell(x_j)]}$$

$$- 2 \sum_i e^{2 \ell(x_i)} \Big\langle \sum_i e^{2 \ell(x_i)} \Big\rangle$$

$$+ \Big\langle \sum_i e^{2 \ell(x_i)} \Big\rangle^2 \Big\rangle$$

$$= \left(\frac{I_o}{N}\right)^2 \{ \sum_i \sum_j < e^{2[\ell(x_i) + \ell(x_j)]} > - \sum_i < e^{2\ell(x_i)} >^2 \}$$

$$= \left(\frac{I_o}{N}\right)^2 \{ \sum_i < e^{4\ell(x_i)} > + 2 \sum_{i \neq j} \sum_j < e^{2[\ell(x_i) + \ell(x_j)]} > - N^2 \}$$

$$= \left(\frac{I_o}{N}\right)^2 \{ Ne^{4\sigma_\ell^2} - N^2 + 2 \sum_{i \neq j} \sum_j < e^{2[\ell(x_i) + \ell(x_j)]} > \}$$

But $< e^{2[\ell(x_i) + \ell(x_j)]} > = \exp \{ 4 <\ell(x)> + 2 <(\ell(x_i) + \ell(x_j) - 2\ell(x)>^2 \}$

$$= \exp \{ 4\eta_\ell + 4C_\ell(0) + 4C_\ell(\rho_{ij}) \}$$

$$= \exp \{ -4\sigma_\ell^2 + 4\sigma_\ell^2 + 4C_\ell(\rho_{ij}) \}$$

$$= e^{4C_\ell(\rho_{ij})}$$

where $C_\ell(\rho_{ij}) = < [\ell(x_i) - <\ell(x_i)>][\ell(x_j) - <\ell(x_j)>] >$

$$\rho_{ij} = |x_i - x_j|$$

and $C_\ell(0) = <[\ell(x) - <\ell(x)>]^2> = \sigma_\ell^2$

Therefore

$$\sigma_{I_1}^2 = \left(\frac{I_o}{N}\right)^2 [Ne^{4\sigma_\ell^2} - N^2 + 2 \sum_{i \neq j} \sum_j e^{4C_\ell(\rho_{ij})}]$$

Note that when $C_\ell(\rho_{ij}) = 0$, $i \neq j$, i.e. uncorrelated,

$$\sum_{i \neq j}^{N} \sum_{j=1}^{N} e^{4C_\ell(\rho_{ij})} = \frac{N(N-1)}{2}$$

and for the uncorrelated case,

$$\sigma_{I_1}^2 = \left(\frac{I_o}{N}\right)^2 [Ne^{4\sigma_\ell^2} - N^2 + N(N-1)]$$

$$= \left(\frac{I_o}{N}\right)^2 [e^{4\sigma_\ell^2} - 1].$$

To find corresponding statistical averages for the nonlinearly weighted case, consider the random variable defined by

$$I_2(x) = \frac{1}{N} \sum_{i=1}^{N} I^2(x_i) = \frac{I_o^2}{N} \sum_{i=1}^{N} e^{4\ell(x_i)} .$$

Then $$\eta_{I_2} = \frac{I_o^2}{N} \sum_i \langle e^{4\ell(x_i)} \rangle$$

$$= I_o^2 e^{4\sigma_\ell^2}$$

$$\sigma_{I_2}^2 = \frac{I_o^4}{N^2} \left\langle \left(\sum_i e^{4\ell(x_i)} - \left\langle \sum_i e^{4\ell(x_i)} \right\rangle \right)^2 \right\rangle$$

$$= \frac{I_o^4}{N^2} \left\{ \sum_i \sum_j e^{4[\ell(x_i) + \ell(x_j)]} - \left[\sum_i \langle e^{4\ell(x_j)} \rangle \right]^2 \right\}$$

$$= \frac{I_o^4}{N^2} \left\{ \sum_i \langle e^{8\ell(x_i)} \rangle - N^2 e^{8\sigma_\ell^2} + 2 \sum_{i \neq j} \sum_j \langle e^{4[\ell(x_i) + \ell(x_j)]} \rangle \right\}$$

$$= \frac{I_o^4}{N^2} \left\{ Ne^{24\sigma_\ell^2} - N^2 e^{8\sigma_\ell^2} + 2 \sum_{i \neq j} \sum_j e^{16C_\ell(\rho_{ij}) + 8\sigma_\ell^2} \right\}$$

When $C_\ell(\rho_{ij}) = 0$, $i \neq j$

$$\sigma_{I_2}^2 = \frac{I_o^4}{N^2} \{Ne^{24\sigma_\ell^2} - N^2 e^{8\sigma_\ell^2} + e^{8\sigma_\ell^2} N(N-1)\}$$

$$= \frac{I_o^4}{N} \{e^{24\sigma_\ell^2} - e^{8\sigma_\ell^2}\}$$

APPENDIX II

Nonlinear Weighting of Diversity Signals*

Consider the case when there is substantial detector noise. This case is approximated by assuming equal levels of Gaussian additive noise in several channels with unequal signal levels. The optimum weighting in this case is to square each signal before adding as is shown in the following analysis.

Consider a system with N channels with the jth channel having a current $i_{s_j} + i_{n_j}$, where i_{s_j} is the signal current and i_{n_j} is the current due to the additive Gaussian noise. The current in the jth channel is weighted by multiplying it by a weighting factor k_j and then all of the channels are added together giving a resultant current of $I_s + I_n$. The final signal-to-noise ratio, ρ_o, of the combination is

$$\rho_o = \frac{I_s^2}{I_n^2} = \frac{\left(\sum_{j=1}^{N} k_j i_{s_j} \right)^2}{\sum_{j=1}^{N} k_j^2 i_{n_j}^2} .$$

For minimum decision error rate, we wish to maximize ρ_o by an optimum choice of k_j. This is accomplished in an adaptive system by sensing the i_{s_j} values and taking appropriate action to produce the correct k_j. To find the optimum k_j, look for extremum:

$$\frac{\partial \rho_o}{\partial k_j} = \frac{2 i_{s_j} \left(\sum_j k_j i_{s_j} \right)}{\sum_j k_j^2 i_{n_j}^2} - \frac{2 i_{n_j}^2 k_j \left(\sum_j k_j i_{s_j} \right)^2}{\left(\sum_j k_j^2 i_{n_j}^2 \right)^2} = 0$$

*The analysis in this Appendix was contributed by Gail Massey, Professor of Applied Physics, Oregon Graduate Center.

From this,

$$i_{s_j} - k_j i_{n_j}^2 \frac{\sum_j k_j i_{s_j}}{\sum_j k_j^2 i_{n_j}^2} = 0 \quad ,$$

or $$i_{s_j} - k_j i_{n_j}^2 \frac{I_s}{I_n^2} = 0 \quad .$$

Then $$k_j = \frac{i_{s_j}}{i_{n_j}^2} \frac{I_n^2}{I_s} \quad .$$

The ratio of the weighted signal current in the jth channel to the total optimized signal current, R_j, is:

$$R_j = \frac{i_{s_j} k_j}{I_s} = \left(\frac{i_{s_j}}{i_{n_j}} \right)^2 \left(\frac{I_n}{I_s} \right)^2$$

$$= \frac{\rho_j}{\rho_o} \quad .$$

Thus, the optimum weighting of the currents is in proportion to their signal-to-noise ratios.

If we assume that the noise in each channel has the same statistics, the optimum combination is in proportion to the signal photocurrent powers in each channel. Thus we want to combine the squares of the signals. If we assume further that $i_{s_j}^2 >> i_{n_j}^2$ for all j, this result can be approximated by squaring the j^{th} total current in each channel, i.e., $(i_{s_j} + i_{n_j})^2 \approx i_{s_j}^2$.

The final optimized signal-to-noise ratio is

$$\rho_o = \frac{\left(\sum_j \frac{i_{s_j}^2}{i_{n_j}^2} \frac{I_n^2}{I_s} \right)^2}{\sum_j \left(\frac{i_{s_j}}{i_{n_j}} \frac{I_n^2}{I_s} \right)^2}$$

$$= \frac{\left[\sum_j \left(\frac{i_{s_j}}{i_{n_j}}\right)^2\right]^2}{\sum_j \left(\frac{i_{s_j}}{i_{n_j}}\right)^2}$$

$$= \sum_j \left(\frac{i_{s_j}}{i_{n_j}}\right)^2$$

$$= \sum_{j=1}^{N} \rho_j$$

Thus, the optimized signal-to-noise ratio is simply the sum of the single channel signal-to-noise ratio.

In order to make a decision on the resulting signal, $(I_s + I_n)$, we note that under adaptive conditions, I_s and I_n both vary. For any set of k_j, I_n is known statistically a priori. Thus the optimum Bayes decision[17] structure is a threshold detector that decides "field is present" when $I_s > \frac{\overline{I}_s}{2} + \frac{\sigma^2}{\overline{I}_s} \ell nK$ and "field is absent" when the opposite inequality is true:

where $K = \frac{q_o C_\alpha}{q_1 C_\beta}$ and,

q_o = probability that field is absent
q_1 = probability that field is present
C_α = cost of deciding field is present when it is not
C_β = cost of deciding field is absent when it is present
σ^2 = noise variance under best weighting.
$\overline{I}_s$ = average over many bits of the combined signal.

In most cases of interest, $q_o = q_1 = \frac{1}{2}$, and $C_\alpha = C_\beta$ (symmetric binary channel), and the inequality used for making a decision becomes

$$I_s \gtrless \frac{\overline{I}_s}{2} .$$

The optimum receiver structure under these conditions then is to square the signal photocurrent before adding. This can be approximated by passing the current in the jth channel (i_{s_j} and i_{n_j}) through an appropriate low pass filter to obtain $\bar{i}_{s_j} = k_j$ and multiplying this times the current in the jth channel to obtain $\bar{i}_{s_j} i_{s_j} + \bar{i}_{s_j} i_{n_j}$, before adding the N channels together. A decision is then made by passing the total current, $I_s + I_n$ through an appropriate low pass filter to obtain $1/2\ \bar{I}_s$ as an adaptive threshold to be used in making the decision.

REFERENCES

1. J.R. Kerr, P.J. Titterton, A.R. Kraemer, C.R. Cooke, "Atmospheric Optical Communications Systems", Proc. IEEE, 58, 1691 (1970).

2. R. Kompfner, "Optics at Bell Laboratories - Optical Communications", Applied Optics, 11, 2412 (1972).

3. R.S. Kennedy, "Communication Through Optical Scattering Channels: An Introduction", Proc. IEEE, 58, 1651 (1970).

4. M. Ross, "Laser Receivers", New York: Wiley, 1966.

5. R.S. Lawrence and J.W. Strohbehn, "A Survey of Clear Air Propagation Effects Relevant to Optical Communication", Proc. IEEE, 58, 1523 (1970).

6. V.I. Tartarski, "Wave Propagation in a Turbulent Medijm", New York, McGraw-Hill, 1966.

7. R.W. Lee, J.C. Harp, "Weak Scattering in Random Media with Applications to Remote Probing", Proc. IEEE, 57, 375 (1969).

8. J.R. Kerr, "Experiments on Turbulence Characteristics and Multiwave Length Scintillation Phenomenon", J.Opt.Soc.Am., 62, 1040 (1972).

9. J.R. Dunphy and J.R. Kerr, "Scintillation Measurements for Large Integrated - Path Turbulence", 3.Opt.Soc.Am., 63, 981 (1973).

10. Appendix (I).

11. D.L. Fried, "Aperture Averaging of Scintillation", J.Opt. Soc. Am., 57, 169 (1967).

12. E.V. Hoversten, R.O. Harger, S.J. Halme, "Communication Theory for the Turbulent Atmosphere", Proc. IEEE, 58, 1626 (1970).

13. T.A. Brackey, "Application of Spatial Diversity to Atmospheric Optical Line-of-Sight Communications Systems," Ohio State University Electro-Science Laboratory Report #2156-12, Appendix J, October 1969.

14. R.L. Mitchell, "Permanence of the Log Normal Distribution," J.Opt.Soc. Am., 58, 1267 (1968).

15. D.L. Fried and F.A. Schmeltzer, "The Effect of Atmospheric Scintillation on an Optical Data Channel - Laser Radar and Binary Communications", Applied Optics, 6, 1729 (1967).

16. These computer programs are available at the computer center of the Oregon Graduate Center.

17. J. Hancock and P. Wintz, "Signal Detection Theory", McGraw-Hill, 1966.